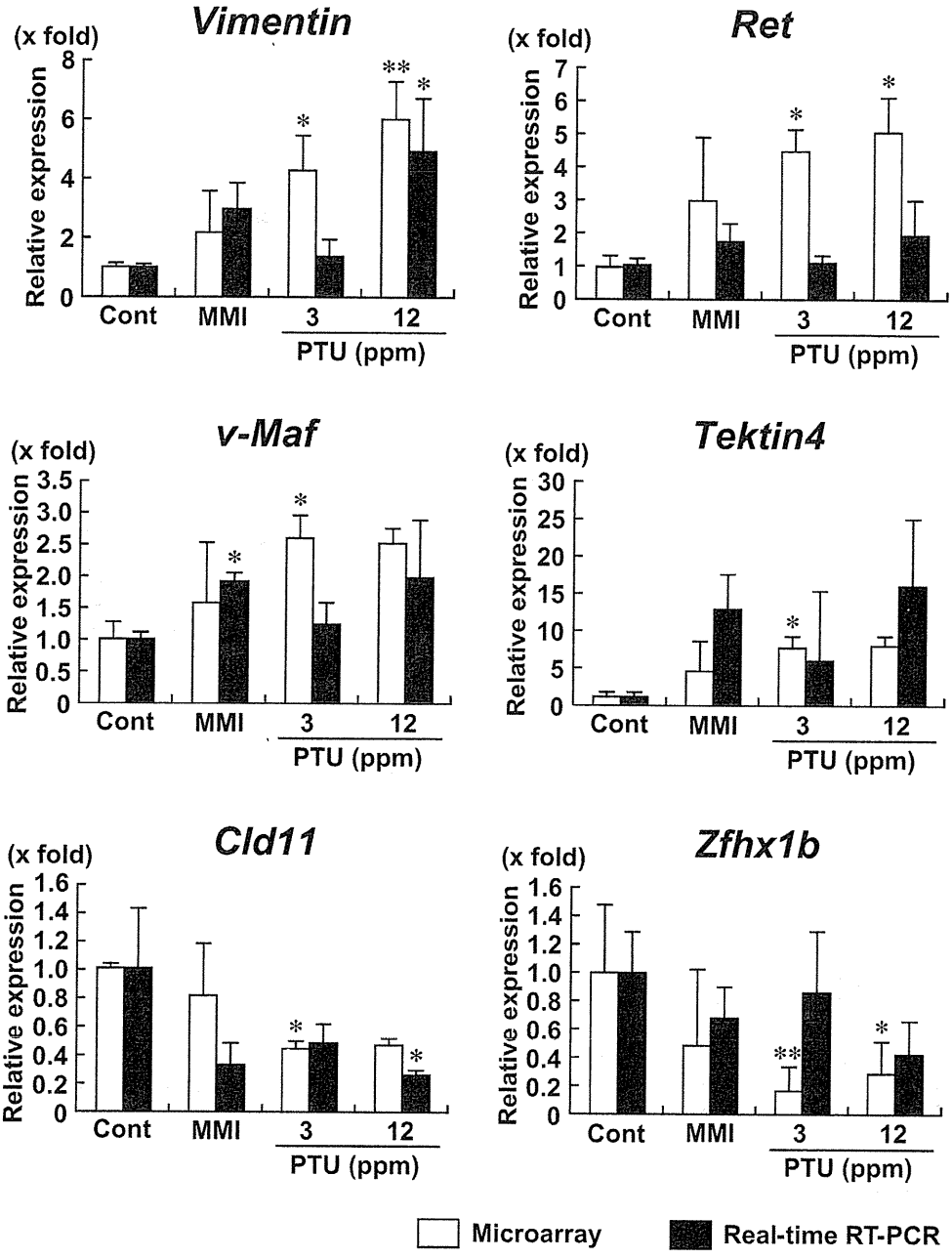

Fig. 3. Validation of mRNA expression of genes selected from microarray data ($n = 4$ in each group). $^{*}P < 0.05$, $^{**}P < 0.01$ vs. untreated controls.

up- or down-regulation in response to 200 ppm MMI was much lower compared with those of both PTU groups. Four hundred and eighty six common genes (428 up-regulated; 58 down-regulated) were identified with altered expression between MMI and both PTU groups (Fig. 2 and Supplementary data: Tables 1 and 2). Among these genes, the genes associated with central nervous system (CNS) development, cell differentiation and cell adhesion were commonly up- or down-regulated in response to anti-thyroid agents (Supplementary data: Tables 1 and 2). Twenty-four genes (20 up-regulated; 4 down-regulated) were related to CNS development involving glial cell differentiation, axon guidance, myelination, and cellular migration (Table 1). Among them, 12 up-regulated genes and two down-regulated genes showed PTU dose-dependent expression changes. For confirmation of microarray data, four genes that were up-regulated and two genes that were down-regulated in response to anti-thyroid agents were selected for mRNA expression analysis by real-time RT-PCR. Results are summarized in Fig. 3. All genes examined showed fluctuations in transcript levels in any of anti-thyroid agent treatment groups, which was similar to that of microarray data.

3.2. Immunolocalization of selected molecules in cerebral white matter

Immunohistochemical localization of vimentin, Ret, DCC and Cld11 was examined in the cerebral white matter. Within white

Please cite this article in press as: Fujimoto H, et al. Increased cellular distribution of vimentin and Ret in the cingulum induced by developmental hypothyroidism in rat offspring maternally exposed to anti-thyroid agents. Reprod Toxicol (2012), http://dx.doi.org/10.1016/j.reprotox.2012.03.005

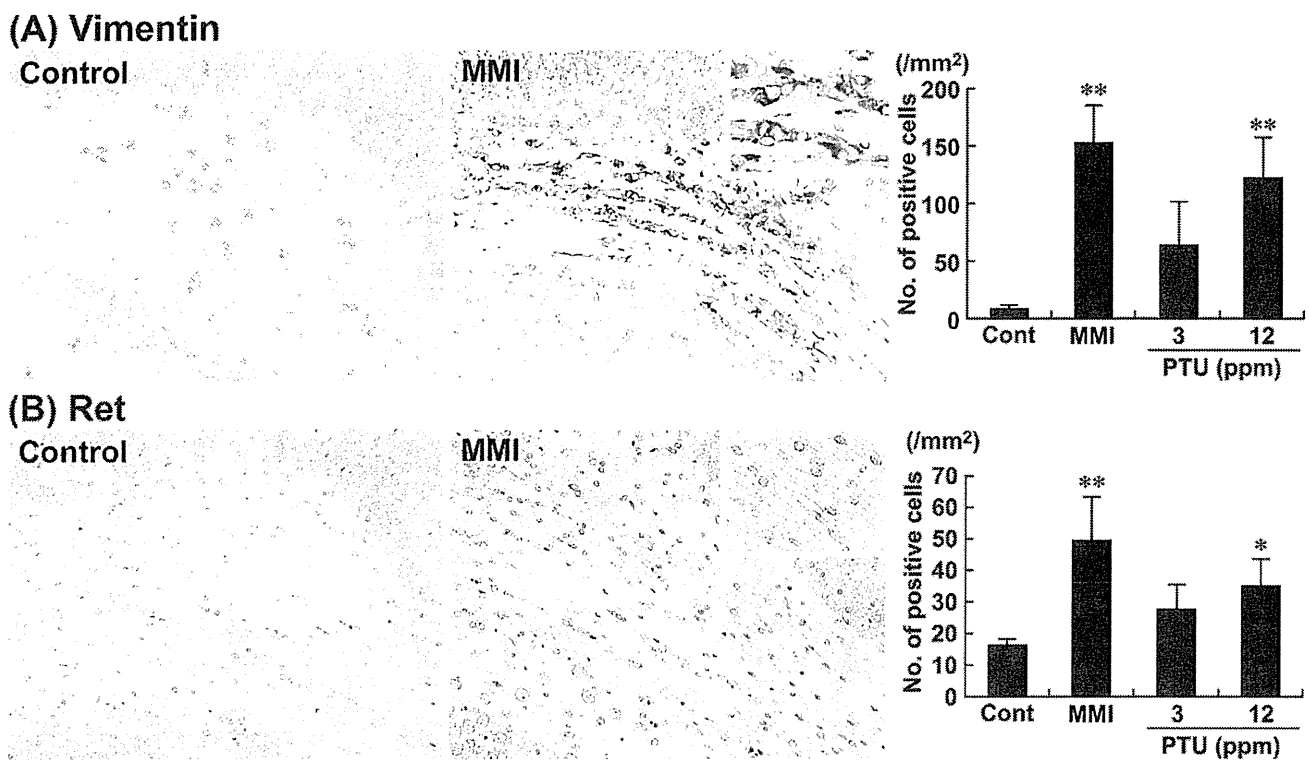

Fig. 4. Immunohistochemical distributions of vimentin- and Ret-positive cells in the while matter tissue. (A) Vimentin-immunoreactive cells in the cingulum. Untreated control animal (left) and MMI-treated animal (right). 200× magnification (inset: 400× magnification). Graph shows the mean number of positive cells within the cingulum at 200× magnification (untreated controls: $n = 6$; MMI and PTU groups: $n = 10$). $^{**}P < 0.01$ vs. untreated controls. (B) Ret-immunoreactive cells in the cingulum. Untreated control animal (left), MMI-treated animal (right). 200× magnification (inset: 400× magnification). Graph shows the mean number of positive cells within the cingulum at 100× magnification (untreated controls: $n = 6$; MMI and PTU groups: $n = 10$). $^{*}P < 0.05$, $^{**}P < 0.01$ vs. untreated controls.

matter tissues, vimentin-immunoreactive cells were scarcely distributed in untreated control animals (Fig. 4A). After treatment with anti-thyroid agents, the distribution of vimentin-positive cells were mainly observed in the cingulum with a statistically significant increase in number with MMI and 12 ppm PTU treatments (Fig. 4A).

Ret-immunoreactive cells were mainly observed in white matter tissues of untreated control animals (Fig. 4B). After treatment with anti-thyroid agents, Ret-positive cells were mainly observed in the cingulum with a statistically significant increase in number with MMI and 12 ppm PTU treatments (Fig. 4B).

DCC showed diffuse immunoreactivity in white matter, indicating myelin sheaths with a statistically significant increase in the intensity scores of animals treated with MMI and 12 ppm PTU as compared with those of the untreated control (Fig. 5A).

Diffuse Cld11-immunoreactivity was observed in white matter, indicating myelin sheaths (Fig. 5B). The immunoreactivity showed a statistically significant increase in the intensity score of animals treated with MMI as compared with that of the untreated control (Fig. 5B).

3.3. Immunolocalization of GFAP

To investigate the cell type of vimentin-positive cells, cellular distribution of GFAP immunoreactivity was analyzed as a marker of astrocytes. Untreated control animals showed scattered distribution of GFAP-immunoreactive cells in cerebral white matter, and the number of GFAP-immunoreactive cells was higher compared with that of vimentin-positive cells. GFAP-immunoreactive cells showed a similar distribution to that of vimentin-immunoreactive cells, with accumulated distribution in the cingulum (Fig. 6). After treatment with anti-thyroid agents, the number of GFAP-positive cells was significantly increased in animals treated with MMI and 12 ppm PTU.

4. Discussion

In our previous study [16], maternal exposure to MMI and PTU induced typical hypothyroidism-related changes in the concentration of thyroid-related hormones, and variability in the distribution of hippocampal CA1 pyramidal neurons due to neuronal mismigration [16]. With regard to thyroid hormone-related changes in functions or structures in glial cell populations, gene expression alternations have been reported in myelin-related protein genes related to oligodendrocytes [20,21], as well as in enzymes or cytoskeletal components related to astrocytes [22–24]. Therefore, both oligodendrocytes and astrocytes could also be the target of developmental hypothyroidism. We, in the above-mentioned study [16], also observed changes in white matter structures with hypoplasia due to impaired oligodendroglial development as previously reported [2,9]. Using the same study samples, we, in the present study, analyzed immunohistochemical distribution of molecules that showed fluctuations in gene expression from microarray analysis of cerebral white matter tissue collected using microdissection targeting oligodendrocytes and astrocytes. This is the first report to use microarray analysis of gene expression changes induced by developmental hypothyroidism in white matter, whereas there have been such approaches for the study of cerebral cortex and hippocampal substructures [15,25,26]. We found that anti-thyroid agents caused fluctuations in a number of genes associated with CNS development involving glial cell differentiation, axon guidance, myelination, and cellular migration as listed in Table 1. Among them, vimentin, Ret, DCC and Cld11

Please cite this article in press as: Fujimoto H, et al. Increased cellular distribution of vimentin and Ret in the cingulum induced by developmental hypothyroidism in rat offspring maternally exposed to anti-thyroid agents. Reprod Toxicol (2012), http://dx.doi.org/10.1016/j.reprotox.2012.03.005

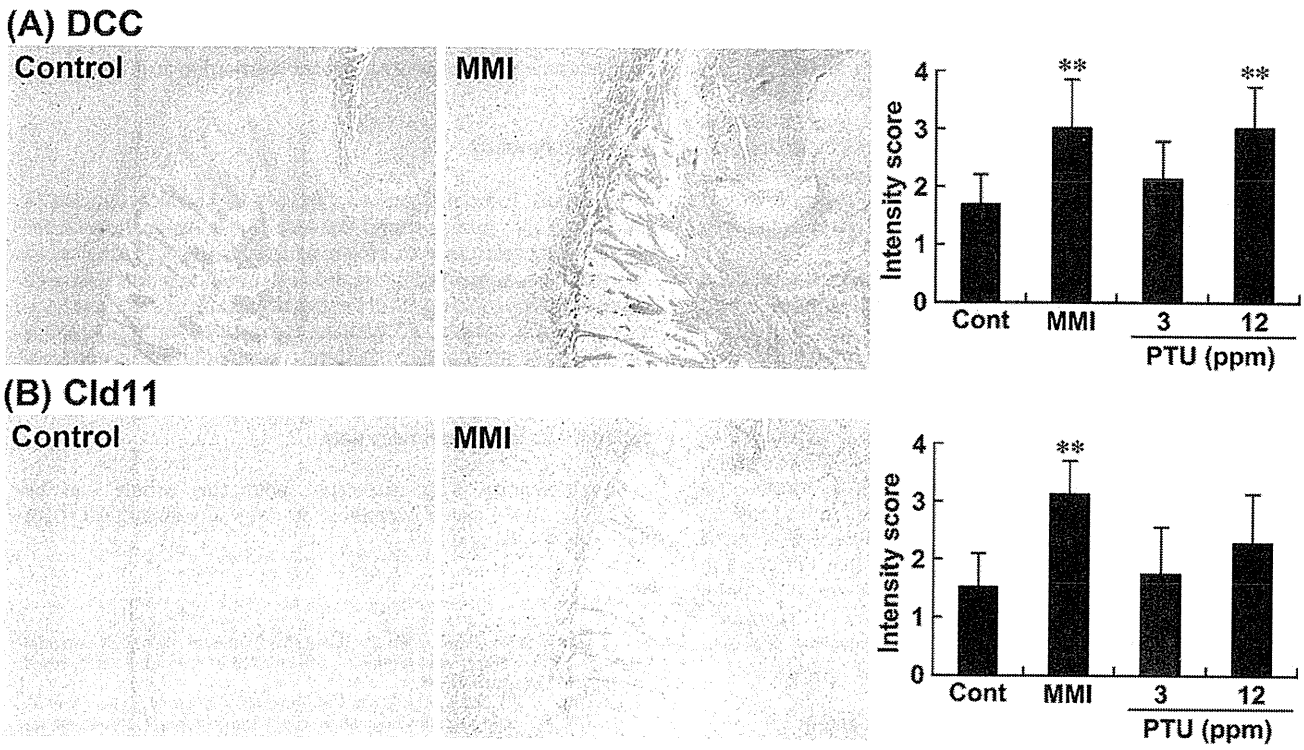

Fig. 5. Immunohistochemical distributions of DCC- and Cld11 in the while matter tissue. (A) DCC-immunoreactivity in the myelin sheath of the external capsule, internal capsule, and fimbria of the hippocampus. Untreated control animal (left), MMI-treated animal (right). 40× magnification. Graph shows the mean intensity score of immunoreactivity at 40× magnification (untreated controls: $n = 6$; MMI and PTU groups: $n = 10$). $^{**}P < 0.01$ vs. untreated controls. (B) Cld11-immunoreactivity in the myelin sheath of the external capsule, internal capsule, and fimbria of the hippocampus. Untreated control animal (left), MMI-treated animal (right). 40× magnification. Graph shows the mean intensity score of immunoreactivity at 40× magnification (untreated controls: $n = 6$; MMI and PTU groups: $n = 10$). $^{**}P < 0.01$ vs. untreated controls.

showed immunohistochemical distribution changes in the cerebral white matter of offspring after maternal exposure to PTU and MMI.

Cld11 is a four-transmembrane protein, which is primarily expressed in oligodendrocytes of the CNS and is the third most abundant CNS myelin protein [27–29]. Cld11 is involved in the formation of intramembranous tight junctions within the myelin sheath [30]. It is known that developmental hypothyroidism results in continued reduction of oligodendrocytes in the CC region from PND 10 [2]. In vitro study has shown that Cld11-overexpression results in induction of oligodendrocyte proliferation [31]. This result indicates that the overexpression of Cld11 at PND 20 is a compensatory response to decrease numbers of oligodendrocytes. However, mRNA levels were inconsistently decreased, suggesting involvement of post-transcriptional events such as those regulating mRNA stability and protein turnover.

DCC is a transmembrane receptor for netrin-1 via the fourth fibronectin type III domain [32]. Netrin-1 is a secreted protein, which elicits both attractive and repulsive responses in axonal guidance, neuronal migration and oligodendroglial migration depending on the homomeric or heteromeric combination of receptor dimers including DCC and Unc5 [33–35]. Netrin-1 signaling via DCC mediates growth cone extension and myelin sheath formation [36,37]. Therefore, increased expression of DCC in the myelin sheath at PND 20 induced by developmental hypothyroidism in the present study suggests a compensatory increase in response to suppression of myelin sheath formation [2]. However,

Fig. 6. Immunohistochemical distributions of GFAP-positive cells in the cingulum. Untreated control animal (left), MMI-treated animal (right). 200× magnification. Graph shows the mean number of positive cells within the cingulum at 200× magnification (untreated controls: $n = 6$; MMI and PTU groups: $n = 10$). $^{*}P < 0.05$, $^{**}P < 0.01$ vs. untreated controls.

Please cite this article in press as: Fujimoto H, et al. Increased cellular distribution of vimentin and Ret in the cingulum induced by developmental hypothyroidism in rat offspring maternally exposed to anti-thyroid agents. Reprod Toxicol (2012), http://dx.doi.org/10.1016/j.reprotox.2012.03.005

DCC has an alternative function to drive cell death independent of both mitochondria-dependent and death receptor/caspase-8 pathways [38,39]. Moreover, DCC induces cell death in the absence of netrin-1 [40]. Because we did not find an increase in netrin-1 transcript levels using microarray analysis, it is possible that increased ligand-free DCC may lead to glial cell apoptosis. Progressive decrease in the CC area and the number of oligodendrocytes in this area during maturation after developmental hypothyroidism suggests the involvement of apoptosis due to increased ligand-free DCC [2,16].

Ret is a receptor protein–tyrosine kinase of glial cell line-derived neurotrophic factor (GDNF), a member of the transforming growth factor-β family [41]. GDNF signals play a critical role in development of the entire nervous system, kidney morphogenesis and spermatogenesis. While the functional relevance of Ret in oligodendrocytes has not been reported, this molecule is expressed in progenitor and immature oligodendrocytes in vitro and mediates cell proliferation induced by GDNF treatment [42]. Therefore, increased expression of Ret on PND 20 proceeding developmental hypothyroidism suggests a compensatory increase in response to decreased numbers of oligodendrocytes [2]. However, Ret induces cell death in the absence of its ligand similar to that of DCC [43]. Because we did not find an increase in GDNF transcript levels using microarray analysis, a progressive decrease in the size of the CC area and its oligodendrocyte density during maturation suggests involvement of apoptosis due to the increase of ligand-free Ret [2,16].

Vimentin is a member of the intermediate filament family of proteins. In the brain, this molecule is expressed in immature astrocytes during development [44–46]. Reactive astrocytes that are activated immature astrocytes during gliosis processes in response to injuries of CNS tissue also express vimentin [47,48]. Reactive astrocytes also express GFAP similar to that of mature astrocytes [47,48], suggesting that immature astrocytes can express both of vimentin and GFAP. On the other hand, developmental hypothyroidism leads to increase in vimentin expression in fetal rat brains [23]. Increase of GFAP-expression was also reported after developmental hypothyroidism in the CC region on PND 15 [49]. These results may suggest that developmental hypothyroidism increases the immature population of astrocytes. In the present study, vimentin-immunoreactive cells showed similar localization to those positive for GFAP. Therefore, a larger population of vimentin-positive cells in the cingulum induced by developmental hypothyroidism was considered to consist of immature astrocytes resembling reactive astrocytes. Interestingly, we previously reported frequent induction of subcortical band heterotopia in the CC, manifested by the appearance of aberrant cortical tissue in this anatomical area, in hypothyroid animals identical to the present study [16]. Anatomical location of this heterotopic tissue was close to the cingulum accumulating immature astrocytes, suggesting an etiological relation between the two. Alternatively, the increased immature astrocytes may simply be the reactive change in response to reduced oligodendrocytes due to developmental hypothyroidism [2,16,49]. However, developmental hypothyroidism may affect differentiation of neuronal progenitor cells, thereby inhibiting differentiation into oligodendrocytes, and instead, facilitating astrocytic differentiation during gliogenesis.

In conclusion, focusing on white matter development, we found aberrant expression of molecules associated with brain development after maternal exposure to anti-thyroid agents. Immunohistochemically, we found increased expression of Cld11, DCC, Ret and vimentin in white matter. Among them, vimentin and Ret were expressed in immature astrocytes and oligodendrocytes, respectively. Both positive cell populations were mainly distributed in the cingulum with the largest area of white matter. Because vimentin- and Ret-positive cells can be quantitatively evaluated, these molecules may be useful markers of glial cells, which respond to developmental exposure to thyroid hormone-disrupting chemicals.

Acknowledgments

We thank Tomomi Morikawa for her technical assistance in conducting the animal study. We also thank Ayako Kaneko for her technical assistance in preparing the histological specimens. This work was supported by Health and Labour Sciences Research Grants (Research on the Risk of Chemical Substances) from the Ministry of Health, Labour and Welfare of Japan. All authors disclose that there are no conflicts of interest that could inappropriately influence the outcome of the present study.

Appendix A. Supplementary data

Supplementary data associated with this article can be found, in the online version, at http://dx.doi.org/10.1016/j.reprotox.2012.03.005.

References

[1] Porterfield SP. Thyroidal dysfunction and environmental chemicals—potential impact on brain development. Environmental Health Perspectives 2000;108(Suppl. 3):433–8.
[2] Schoonover CM, Seibel MM, Jolson DM, Stack MJ, Rahman RJ, Jones SA, et al. Thyroid hormone regulates oligodendrocyte accumulation in developing rat brain white matter tracts. Endocrinology 2004;145:5013–20.
[3] Montero-Pedrazuela A, Venero C, Lavado-Autric R, Fernández-Lamo I, García-Verdugo JM, Bernal J, et al. Modulation of adult hippocampal neurogenesis by thyroid hormones: implications in depressive-like behavior. Molecular Psychiatry 2006;11:361–71.
[4] de Escobar GM, Obregón MJ, del Rey FE. Iodine deficiency and brain development in the first half of pregnancy. Public Health Nutrition 2007;10:1554–70.
[5] Comer CP, Norton S. Effects of perinatal methimazole exposure on a developmental test battery for neurobehavioral toxicity in rats. Toxicology and Applied Pharmacology 1982;63:133–41.
[6] Akaike M, Kato N, Ohno H, Kobayashi T. Hyperactivity and spatial maze learning impairment of adult rats with temporary neonatal hypothyroidism. Neurotoxicology and Teratology 1991;13:317–22.
[7] Guadaño Ferraz A, Escobar del Rey F, Morreale de Escobar G, Innocenti GM, Berbel P. The development of the anterior commissure in normal and hypothyroid rats. Brain Research Developmental Brain Research 1994;81:293–308.
[8] Lavado-Autric R, Ausó E, García-Velasco JV, Arufe Mdel C, Escobar del Rey F, Berbel P, et al. Early maternal hypothyroxinemia alters histogenesis and cerebral cortex cytoarchitecture of the progeny. Journal of Clinical Investigation 2003;111:954–7.
[9] Goodman JH, Gilbert ME. Modest thyroid hormone insufficiency during development induces a cellular malformation in the corpus callosum: a model of cortical dysplasia. Endocrinology 2007;148:2593–7.
[10] Shibutani M, Uneyama C, Miyazaki K, Toyoda K, Hirose M. Methacarn fixation: a novel tool for analysis of gene expressions in paraffin-embedded tissue specimens. Laboratory Investigation 2000;80:199–208.
[11] Uneyama C, Shibutani M, Masutomi N, Takagi H, Hirose M. Methacarn fixation for genomic DNA analysis in microdissected, paraffin-embedded tissue specimens. Journal of Histochemistry and Cytochemistry 2002;50:1237–45.
[12] Takagi H, Shibutani M, Kato N, Fujita H, Lee KY, Takigami S, et al. Microdissected region-specific gene expression analysis with methacarn-fixed, paraffin-embedded tissues by real-time RT-PCR. Journal of Histochemistry and Cytochemistry 2004;52:903–13.
[13] Shibutani M, Lee KY, Igarashi K, Woo GH, Inoue K, Nishimura T, et al. Hypothalamus region-specific global gene expression profiling in early stages of central endocrine disruption in rat neonates injected with estradiol benzoate or flutamide. Developmental Neurobiology 2007;67:253–69.
[14] Woo GH, Takahashi M, Inoue K, Fujimoto H, Igarashi K, Kanno J, et al. Cellular distributions of molecules with altered expression specific to thyroid proliferative lesions developing in a rat thyroid carcinogenesis model. Cancer Science 2009;100:617–25.
[15] Saegusa Y, Woo GH, Fujimoto H, Inoue K, Takahashi M, Hirose M, et al. Gene expression profiling and cellular distribution of molecules with altered expression in the hippocampal CA1 region after developmental exposure to anti-thyroid agents in rats. Journal of Veterinary Medical Science 2010;72:187–95.
[16] Shibutani M, Woo GH, Fujimoto H, Saegusa Y, Takahashi M, Inoue K, et al. Assessment of developmental effects of hypothyroidism in rats from in utero and lactation exposure to anti-thyroid agents. Reproductive Toxicology 2009;28:297–307.

Please cite this article in press as: Fujimoto H, et al. Increased cellular distribution of vimentin and Ret in the cingulum induced by developmental hypothyroidism in rat offspring maternally exposed to anti-thyroid agents. Reprod Toxicol (2012), http://dx.doi.org/10.1016/j.reprotox.2012.03.005

[17] Masutomi N, Shibutani M, Takagi H, Uneyama C, Takahashi N, Hirose M. Impact of dietary exposure to methoxychlor, genistein, or diisononyl phthalate during the perinatal period on the development of the rat endocrine/reproductive systems in later life. Toxicology 2003;192:149–70.
[18] Nakamura R, Teshima R, Hachisuka A, Sato Y, Takagi K, Nakamura R, et al. Effects of developmental hypothyroidism induced by maternal administration of methimazole or propylthiouracil on the immune system of rats. International Immunopharmacology 2007;7:1630–8.
[19] Lee KY, Shibutani M, Inoue K, Kuroiwa K, U M, Woo GH, et al. Methacarn fixation—effects of tissue processing and storage conditions on detection of mRNAs and proteins in paraffin-embedded tissues. Analytical Biochemistry 2006;351:36–43.
[20] Ibarrola N, Rodríguez-Peña A. Hypothyroidism coordinately and transiently affects myelin protein gene expression in most rat brain regions during postnatal development. Brain Research 1997;752:285–93.
[21] Barradas PC, Vieira RS, De Freitas MS. Selective effect of hypothyroidism on expression of myelin markers during development. Journal of Neuroscience Research 2001;66:254–61.
[22] Farwell AP, Dubord-Tomasetti SA. Thyroid hormone regulates the expression of laminin in the developing rat cerebellum. Endocrinology 1999;140:4221–7.
[23] Evans IM, Pickard MR, Sinha AK, Leonard AJ, Sampson DC, Ekins RP. Influence of maternal hyperthyroidism in the rat on the expression of neuronal and astrocytic cytoskeletal proteins in fetal brain. Journal of Endocrinology 2002;175:597–604.
[24] Dasgupta A, Das S, Sarkar PK. Thyroid hormone promotes glutathione synthesis in astrocytes by up regulation of glutamate cysteine ligase through differential stimulation of its catalytic and modulator subunit mRNAs. Free Radical Biology and Medicine 2007;42:617–26.
[25] Royland JE, Parker JS, Gilbert ME. A genomic analysis of subclinical hypothyroidism in hippocampus and neocortex of the developing rat brain. Journal of Neuroendocrinology 2008;20:1319–38.
[26] Kobayashi K, Akune H, Sumida K, Saito K, Yoshioka T, Tsuji R. Perinatal exposure to PTU decreases expression of Arc, Homer 1, Egr 1 and Kcna 1 in the rat cerebral cortex and hippocampus. Brain Research 2009;1264:24–32.
[27] Bronstein JM, Popper P, Micevych PE, Farber DB. Isolation and characterization of a novel oligodendrocyte-specific protein. Neurology 1996;47:772–8.
[28] Bronstein JM, Micevych PE, Chen K. Oligodendrocyte-specific protein (OSP) is a major component of CNS myelin. Journal of Neuroscience Research 1997;50:713–20.
[29] Morita K, Sasaki H, Fujimoto K, Furuse M, Tsukita S. Claudin-11/OSP-based tight junctions of myelin sheaths in brain and Sertoli cells in testis. Journal of Cell Biology 1999;145:579–88.
[30] Gow A, Southwood CM, Li JS, Pariali M, Riordan GP, Brodie SE, et al. CNS myelin and sertoli cell tight junction strands are absent in Osp/claudin-11 null mice. Cell 1999;99:649–59.
[31] Tiwari-Woodruff SK, Buznikov AG, Vu TQ, Micevych PE, Chen K, Kornblum HI, et al. OSP/claudin-11 forms a complex with a novel member of the tetraspanin super family and beta1 integrin and regulates proliferation and migration of oligodendrocytes. Journal of Cell Biology 2001;153:295–305.
[32] Kruger RP, Lee J, Li W, Guan KL. Mapping netrin receptor binding reveals domains of Unc5 regulating its tyrosine phosphorylation. Journal of Neuroscience 2004;24:10826–34.
[33] Serafini T, Colamarino SA, Leonardo ED, Wang H, Beddington R, Skarnes WC, et al. Netrin-1 is required for commissural axon guidance in the developing vertebrate nervous system. Cell 1996;87:1001–14.
[34] Alcántara S, Ruiz M, De Castro F, Soriano E, Sotelo C. Netrin 1 acts as an attractive or as a repulsive cue for distinct migrating neurons during the development of the cerebellar system. Development 2000;127:1359–72.
[35] Spassky N, de Castro F, Le Bras B, Heydon K, Quéraud-LeSaux F, Bloch-Gallego E, et al. Directional guidance of oligodendroglial migration by class 3 semaphorins and netrin-1. Journal of Neuroscience 2002;22:5992–6004.
[36] Fazeli A, Dickinson SL, Hermiston ML, Tighe RV, Steen RG, Small CG, et al. Phenotype of mice lacking functional Deleted in colorectal cancer (Dcc) gene. Nature 1997;386:796–804.
[37] Rajasekharan S, Baker KA, Horn KE, Jarjour AA, Antel JP, Kennedy TE. Netrin 1 and Dcc regulate oligodendrocyte process branching and membrane extension via Fyn and RhoA. Development 2009;136:415–26.
[38] Forcet C, Ye X, Granger L, Corset V, Shin H, Bredesen DE, et al. The dependence receptor DCC (deleted in colorectal cancer) defines an alternative mechanism for caspase activation. Proceedings of the National Academy of Sciences of the United States of America 2001;98:3416–21.
[39] Furne C, Corset V, Hérincs Z, Cahuzac N, Hueber AO, Mehlen P. The dependence receptor DCC requires lipid raft localization for cell death signaling. Proceedings of the National Academy of Sciences of the United States of America 2006;103:4128–33.
[40] Mehlen P, Rabizadeh S, Snipas SJ, Assa-Munt N, Salvesen GS, Bredesen DE. The DCC gene product induces apoptosis by a mechanism requiring receptor proteolysis. Nature 1998;395:801–4.
[41] Sariola H, Saarma M. Novel functions and signalling pathways for GDNF. Journal of Cell Science 2003;116:3855–62.
[42] Strelau J, Unsicker K. GDNF family members and their receptors: expression and functions in two oligodendroglial cell lines representing distinct stages of oligodendroglial development. Glia 1999;26:291–301.
[43] Bordeaux MC, Forcet C, Granger L, Corset V, Bidaud C, Billaud M, et al. The RET proto-oncogene induces apoptosis: a novel mechanism for Hirschsprung disease. EMBO Journal 2000;19:4056–63.
[44] Pixley SK, de Vellis J. Transition between immature radial glia and mature astrocytes studied with a monoclonal antibody to vimentin. Brain Research 1984;317:201–9.
[45] Ciesielski-Treska J, Goetschy JF, Ulrich G, Aunis D. Acquisition of vimentin in astrocytes cultured from postnatal rat brain. Journal of Neurocytology 1988;17:79–86.
[46] Alonso G. Proliferation of progenitor cells in the adult rat brain correlates with the presence of vimentin-expressing astrocytes. Glia 2001;34:253–66.
[47] Pekny M, Wilhelmsson U, Bogestål YR, Pekna M. The role of astrocytes and complement system in neural plasticity. International Review of Neurobiology 2007;82:95–111.
[48] Eddleston M, Mucke L. Molecular profile of reactive astrocytes—implications for their role in neurologic disease. Neuroscience 1993;54:15–36.
[49] Sharlin DS, Bansal R, Zoeller RT. Polychlorinated biphenyls exert selective effects on cellular composition of white matter in a manner inconsistent with thyroid hormone insufficiency. Endocrinology 2006;147:846–58.

Please cite this article in press as: Fujimoto H, et al. Increased cellular distribution of vimentin and Ret in the cingulum induced by developmental hypothyroidism in rat offspring maternally exposed to anti-thyroid agents. Reprod Toxicol (2012), http://dx.doi.org/10.1016/j.reprotox.2012.03.005

G Model
RTX 66861-12
ARTICLE IN PRESS

Reproductive Toxicology xxx (2012) xxx–xxx

Contents lists available at SciVerse ScienceDirect

Reproductive Toxicology

journal homepage: www.elsevier.com/locate/reprotox

Reversible aberration of neurogenesis affecting late-stage differentiation in the hippocampal dentate gyrus of rat offspring after maternal exposure to manganese chloride

Takumi Ohishi[a,b], Liyun Wang[a], Hirotoshi Akane[a], Ayako Shiraki[a], Ken Goto[b], Yoshiaki Ikarashi[c], Kazuhiko Suzuki[a], Kunitoshi Mitsumori[a], Makoto Shibutani[a,*]

[a] Laboratory of Veterinary Pathology, Tokyo University of Agriculture and Technology, 3-5-8 Saiwai-cho, Fuchu-shi, Tokyo 183-8509, Japan
[b] Gotemba Laboratory, Bozo Research Center Inc., 1284 Kamado, Gotemba-shi, Shizuoka 412-0039, Japan
[c] Division of Environmental Chemistry, National Institute of Health Sciences, 1-18-1 Kamiyoga, Setagaya-ku, Tokyo 158-8501, Japan

ARTICLE INFO

Article history:
Received 13 November 2011
Received in revised form 15 March 2012
Accepted 25 April 2012
Available online xxx

Keywords:
Manganese
Developmental neurotoxicity
Hippocampal dentate gyrus
Thyroid hormone

ABSTRACT

To examine the effects of developmental manganese (Mn)-exposure on hippocampal neurogenesis, pregnant rats were treated with $MnCl_2 \cdot 4H_2O$ in the diet at 32, 160 or 800 ppm from gestation day 10 to day 21 after delivery. Serum concentrations of thyroid-related hormones were examined in offspring exposed to $MnCl_2 \cdot 4H_2O$ at 800 or 1600 ppm. Immunohistochemical analysis revealed increased doublecortin-positive cells in the subgranular zone of the dentate gyrus on postnatal day (PND) 21 following exposure to $MnCl_2 \cdot 4H_2O$ at 800 ppm, indicating an increase of type-3 progenitor or immature granule cells. Reelin-positive cells, suggestive of γ-aminobutyric acid-ergic interneurons in the dentate hilus, also increased at 800 ppm on PND 21. Brain Mn concentrations increased in offspring on PND 21 at 160 and 800 ppm, whereas brain concentrations in the dams were unchanged. Serum concentrations of triiodothyronine and thyroxine decreased at 800 and 1600 ppm, whereas thyroid-stimulating hormone increased only after exposure at 800 ppm. All changes disappeared on PND 77. Thus, maternal exposure to $MnCl_2 \cdot 4H_2O$ at 800 ppm mildly and reversibly affects neurogenesis targeting late-stage differentiation in the hippocampal dentate gyrus of rat offspring. Direct effects of accumulated Mn in the developing brain might be implicated in the mechanism of the development of aberrations in neurogenesis; however, indirect effects through thyroid hormone fluctuations might be rather minor.

1. Introduction

Manganese (Mn) is known as an essential trace metal and is needed for normal immune function, regulation of blood sugar and cellular energy, reproduction, digestion, bone growth, and aid in the defense mechanisms against free radicals [1]. Although natural Mn deficiency is rare, Mn-induced neurotoxicity by excess exposure known as manganism is similar to Parkinson's disease and has been well described [2,3].

Estimated safe and adequate daily dietary intake (ESADDI) of Mn has been estimated at approximately 0.6 mg/day for individuals 7–12 months of age, 1.2 mg/day for those 1–3 years of age, 1.5 mg/day for those 4–8 years of age and 2–5 mg/day for adults. On the other hand, the ESADDI for newborns has been estimated to be less than that for adults or children at 0.003 mg/day [1,3]. Several experimental studies have found that neonatal animals were more sensitive to Mn-induced neurotoxicity than adult animals in behavioral tests and on brain neurochemistry [4]. However, the risk of Mn-induced neurotoxicity during both pre- and postnatal periods has received relatively little attention and there are few studies using histopathological evaluation.

It has been suggested that Mn might also affect thyroid hormone homeostasis [5]. Thyroid hormones are critically involved in the growth, development and function of the central nervous system [6]. Using a rat model of developmental hypothyroidism, we have recently detected an increase of reelin-expressing γ-aminobutyric acid (GABA)ergic interneurons displaying an immature phenotype in the dentate hilus that was sustained through to the adult stage, as well as increased apoptosis and decreased cell proliferation

Abbreviations: DCX, doublecortin; ESADDI, estimated safe and adequate daily dietary intake; GABA, γ-aminobutyric acid; GAD67, glutamic acid decarboxylase 67; GD, gestation day; GFAP, glial fibrillary acidic protein; Mn, manganese; NeuN, neuron-specific nuclear protein; PCNA, proliferating cell nuclear antigen; PND, postnatal day; SGZ, subgranular zone; Tbr2, T box brain 2; TSH, thyroid-stimulating hormone; TUNEL, terminal deoxynucleotidyl transferase dUTP nick end labeling; T_3, triiodothyronine; T_4, thyroxine.

* Corresponding author. Tel.: +81 42 367 5874; fax: +81 42 367 5771.
E-mail address: mshibuta@cc.tuat.ac.jp (M. Shibutani).

0890-6238/$ – see front matter © 2012 Elsevier Inc. All rights reserved.
http://dx.doi.org/10.1016/j.reprotox.2012.04.009

Table 1
Culling and number of animals examined in Experiment 1.

	Per litter	Per group (dams = 8)
PND 4		
Culling	Kept 4 males and 4 females	Kept 32 males and 32 females
PND 21		
Animals subjected to necropsy	2 males and 2 females	16 males and 16 females
Immunohistochemical analysis	1 or 2 males	10 males
Analyses of Mn concentrations and real-time RT-PCR	1 male	6 males
PND 77		
Animals subjected to necropsy	2 males and 2 females	16 males and 16 females
Immunohistochemical analysis	1 or 2 males	10 males
Analysis of Mn concentrations	1 male	6 males

Abbreviation: PND, postnatal day.

suggestive of impaired neurogenesis in the neuroblast-producing subgranular zone (SGZ) [7]. Thus, the concern about effects on neurogenesis associated with changes in thyroid-related hormones arises in the case of developmental Mn-exposure.

Within the hippocampal formation, the dentate gyrus is a unique structure that can continue neurogenesis throughout the lifetime and that is a well-known target of developmental hypothyroidism [8]. The dentate gyrus is crucial for higher brain functions such as learning and memory, and malformation and malfunction of the dentate gyrus are associated with neurological and psychiatric disorders [9]. The dentate gyrus is known for its ongoing neurogenesis at the SGZ throughout postnatal life [10,11], and GABAergic interneurons in the hilus can control neurogenesis [7,12]. Reelin is a secreted extracellular matrix glycoprotein that plays a critical role in neuronal migration and positioning during brain development [13]. During the early postnatal life, reelin expression becomes established in a subpopulation of GABAergic interneurons in the dentate gyrus, with a high density in the hilus and along the base of the granule cell layer [14], where reelin is maintained throughout adult life [15,16]. In the interneurons, reelin modulates dentate granule cell progenitor migration to maintain normal dentate granule cell integration in the neonatal and adult mammalian dentate gyrus [17].

Reproduction studies and developmental neurotoxicity studies require large numbers of animals for detection of subtle dose–response changes. However, for screening purposes of many new chemicals, smaller scale studies, preferably with short-term experiments, need to be established. To establish a rapid screening system for developmental neurotoxicants, we focused on the neurogenesis and its regulatory system in the dentate gyrus using rodent models [7,18]. We hypothesize that monitoring of the dentate gyrus may provide a valuable tool for the detection of developmental neurotoxicants.

In the present study, to elucidate the effects of developmental exposure to Mn on neurogenesis, distribution of granule cell lineages as well as their proliferation and apoptosis in the SGZ and reelin-producing interneurons in the hilus of the hippocampal dentate gyrus were analyzed in the offspring of rats exposed to Mn during pregnancy and lactation periods in a small scale animal study. Furthermore, to clarify the relation of thyroid function to the Mn-induced brain effect, serum concentrations of thyroid-related hormones were also analyzed in Mn-exposed offspring.

2. Materials and methods

2.1. Chemicals and animals

Manganese chloride tetrahydrate ($MnCl_2{\cdot}4H_2O$; CAS No. 13446-34-9) was purchased from Sigma–Aldrich Japan K.K. (Tokyo, Japan). Pregnant Crl:CD®(SD) rats were purchased from Charles River Japan Inc. (Yokohama, Japan) at gestation day (GD) 1 (appearance of vaginal plugs was designated as GD 0). Pregnant rats were housed individually in mesh cages in an air-conditioned animal room (temperature: 23 ± 2 °C; relative humidity: 45 ± 10%) with a 12-h light/dark cycle and allowed *ad libitum* access to food and tap water. Pregnant rats were then housed individually in plastic cages with wood chip bedding from GD 17, and after delivery, dams with their litter were similarly housed to postnatal day (PND) 21 (where PND 0 is the day of delivery). Dams and pups were allowed *ad libitum* access to food and tap water. Pregnant rats were fed a CRF-1 basal diet (Oriental Yeast Co., Ltd.) from GD 1 to GD 10. All offspring consumed the CRF-1 basal diet and tap water *ad libitum* from PND 21 onwards. Mn concentration in the basal diet was 7.27 mg/100 g and that of the tap water was below the lower detection limit.

All procedures of this study were conducted in compliance with the *Guidelines for Proper Conduct of Animal Experiments* (Science Council of Japan, June 1, 2006) and according to the protocol approved by the Animal Care and Use Committee at BOZO Research Center Inc. All efforts were made to minimize animal suffering.

2.2. Experimental design

2.2.1. Preliminarily dose finding study

A dose finding study was performed based on the dose range report by others [4]. With doses at the level of 0, 500 or 800 ppm (as $MnCl_2{\cdot}4H_2O$) in the basal diet, dams ($n = 3$/dose) were treated from GD 10 to PND 21. As a result, pups exposed to 800 ppm exhibited a slightly decreased body weight, but dams showed no effects in body weight or food consumption (data not shown).

2.2.2. Experiment 1

Based on the results of preliminarily dose finding study, high dose was set at 800 ppm. Dams were randomly divided into four groups including untreated controls. Eight dams per group were treated with 0 (untreated control), 32, 160 or 800 ppm (as $MnCl_2{\cdot}4H_2O$) in the CRF-1 basal diet from GD 10 to PND 21.

Body weight and food consumption of dams were measured throughout the experimental period. The culling and selection of offspring at necropsy are summarized in Table 1. On PND 4, the litters were culled randomly, leaving four male and four female offspring per dam. The offspring were weighed at 3- or 4-day intervals. On PND 21, 16 male and 16 female offspring (two males and two females per dam) per group were subjected to pre-pubertal necropsy for the immunohistochemistry and apoptotic cell detection (10 males and 10 females per group with at least one male and one female per dam), determination of Mn concentration in the brain and real-time reverse transcription polymerase chain reaction (RT-PCR) analysis (six males and six females per group).

The remaining animals were kept through PND 77 and their body weights and food consumption were measured weekly. All offspring consumed the CRF-1 basal diet and tap water *ad libitum* from PND 21 onwards. On PND 77, 16 male and 16 female offspring (two males and two females per dam) per group were subjected to terminal necropsy for immunohistochemistry and apoptotic cell detection (10 males and 10 females per group with at least one male and one female per dam) and determination of Mn concentrations in the brain (six males and six females per group).

At both PND 21 and PND 77, female samples were only preserved without subject to further analysis.

External differentiation on landmarks of physical development was examined with regard to pinna detachment on PND 4, eruption of lower incisor on PND 11 and 14, opening of eyelid on PND 14 and 17, opening of vagina on PND 35 and 42, and cleavage of the balanopreputial gland on PND 42 and 49.

At necropsies of offspring on PND 21 and 77, weights of the brain, liver, kidneys, testes and ovaries were measured. All animals used in the present study were sacrificed by exsanguination from the abdominal aorta under deep anesthesia with ether.

2.2.3. Experiment 2

To evaluate the effects of developmental exposure to $MnCl_2{\cdot}4H_2O$ on the serum concentrations of thyroid related hormones, additional experiments were performed. Dams were randomly divided into three groups including untreated controls. Six dams per group were treated with Mn at 800 or 1600 ppm (as $MnCl_2{\cdot}4H_2O$) in the CRF-1 basal diet from GD 10 to PND 21. On PND 4, the litters were culled randomly, leaving four male and four female offspring per dam. On PND 21, all dams and 10 male offspring per group from six dams (one or two males per dam) were

Please cite this article in press as: Ohishi T, et al. Reversible aberration of neurogenesis affecting late-stage differentiation in the hippocampal dentate gyrus of rat offspring after maternal exposure to manganese chloride. Reprod Toxicol (2012), http://dx.doi.org/10.1016/j.reprotox.2012.04.009

subjected to laparotomy under ether anesthesia and blood samples were collected from the abdominal aorta for hormone analysis. Ten males from the remaining animals (one or two males per dam) were kept through PND 77 and subjected to blood sample collection for hormone analysis on PND 77. After blood sampling, all animals were sacrificed by exsanguination from the abdominal aorta under deep anesthesia with ether.

2.3. Determination of Mn concentration in the brain

To measure Mn concentrations, the cerebellums of all dams and male and female offspring on PND 21 and 77 ($n = 6$/group for each stage) were removed, weighed, frozen in liquid nitrogen and stored at −80 °C until analysis. Samples of dams and male offspring were subjected to analysis (Table 1). Frozen cerebellar tissue was digested using a microwave oven (MARS5, CEM Corp., Matthews, NC, USA); the digested samples were analyzed using inductively coupled plasma mass spectrometer (ICP-MS, HP-7500; Hewlett-Packard Co., Palo Alto, CA, USA) with the monitoring mass of m/z as 55 for Mn.

2.4. Hormone analysis

Blood samples were collected from the abdominal aorta under anesthesia. Serum was prepared and stored at −80 °C. Thyroid-stimulating hormone (TSH), triiodothyronine (T_3) and thyroxine (T_4) concentrations were measured by the chemiluminescent enzyme immunoassay method with the use of DPC IMMULYZE (Siemens Healthcare Diagnostics Inc., IL, USA).

2.5. Behavioral examinations

During the lactation period, sensory and reflex functional examination was conducted for two male and two female offspring in each litter. After weaning, detailed clinical observations, manipulative testing, measurement of grip strength, measurement of motor activity and water-filled multiple T-maze tests were conducted for one male and one female offspring in each litter. The method of each examination is described as follows.

2.5.1. Sensory and reflex functional examinations

Surface righting reflex was examined on PND 10 and was measured as the time required to return to a normal position. Air righting reflex was examined on PND 15 and pupillary reflex, Preyer's reflex and pain reflex were examined on PND 21. The air righting reflex was assessed to examine the normal landing response of an animal to right itself from an inverted position in free fall of about 300 mm height. The pupillary reflex was assessed to examine the normal miotic response to the light. The Preyer's reflex was assessed to examine the normal pinna or startle response to the sound of the Galton's whistle. The pain reflex was assessed to examine the normal response such as avoiding and vocalization to the pinching stimuli of the tail.

2.5.2. Detailed clinical observations

Detailed clinical observations were conducted on PND 29, 43 and 71. In home cage observations, animals were observed for posture, convulsion and abnormal behavior. During handling, animals were observed for ease of removal from cage, fur condition, skin, secretions of the eyes and nose, exophthalmos, palpebral closure, visible mucosal membranes, autonomic nervous functions (lacrimation, piloerection, pupil size, salivation, abnormal respiration), and vocalization and reactivity to handling.

2.5.3. Manipulative testing

Following the detailed clinical observations on PND 71, animals were examined for auditory response, visual approach response, touch response, tail pinch response, pupillary reflex (light reflex), air righting reflex and measured landing foot splay (hind foot).

The auditory response was assessed to examine the normal startle response to clackety-clack stimuli. The visual approach response was assessed to examine the normal response such as sniffing or avoiding to the pen approaching the nose. The touch response was assessed to examine the normal response such as avoiding or soft vocalization to the pen touching the abdomen. The tail pinch response was assessed to examine the normal response such as quick avoiding and vocalization. The pupillary reflex and air righting reflex were assessed as mentioned above.

2.5.4. Grip strength

Following the manipulative testing on PND 71, grip strengths of the forelimbs and hind limbs were measured using a CPU gauge MODEL-RX-5 (Aikoh Engineering Co., Ltd., Osaka, Japan).

2.5.5. Motor activity

Following the measurement of grip strength on PND 71, motor activity was measured using an experimental animal motor activity sensor NS-AS01 (NeuroScience Inc., Tokyo, Japan). The length of measurement was 1 h. Values of 10-min intervals and the 0–60-min value were recorded.

2.5.6. Water-filled multiple T-maze testing

To assess the learning ability, examination in water-filled multiple T-maze (Biel's type) as shown in Supplementary Fig. 1 [19,20] was performed from PND 55 to 57. In this test, animals were subjected to a series of right/left choices to get from one end of the water-filled maze to find the escape. Elapsed time to reach the goal and error counts (number of times the whole body entered into the error area) were measured in three trials each day. The interval of each trial was approximately 5–10 min. The maximum elapsed time for each trial was set at 3 min, and the trials where animals did not reach the goal within 3 min were excluded from statistical analysis. On the 1st day, 1 male in the untreated controls and 1 male in the 160 ppm group at the 1st trial, 1 female in the untreated controls and 1 female in the 800 ppm group at the 2nd trial and 1 female in the untreated controls in the 3rd trial did not reach the goal; however, there were no differences in the number of unreached animals between the untreated controls and any of the treatment groups. Unreached animal data were excluded from the analysis.

One day before the initiation of T-maze test, animals were subjected to examination of swimming ability using a straight course as shown in Supplementary Fig. 1. Elapsed time required to reach the goal was recorded in three trials. There were no differences in the elapsed time using the straight course in both sexes at all doses, indicating no effects on swimming ability (Supplementary Table 1).

2.6. Immunohistochemistry and apoptotic cell detection

The brains of the male offspring sacrificed at PND 21 and 77 were fixed in Bouin's solution at room temperature overnight. Ten male animals from eight dams (one or two males per dam) per group were subjected to analysis at each time point. Coronal slices at the positions of −3.0 and −3.5 mm from the bregma were prepared from the PND 21 and 77 brains, respectively. Brains were routinely processed by paraffin embedding and sectioned at 3 μm.

For immunohistochemistry studies, the brain sections were incubated at 4 °C overnight with antibodies against doublecortin (DCX, rabbit IgG, 1:1000, Abcam, Cambridge, UK), a microtubule binding protein that is expressed in the type-2b and type-3 progenitor cells and immature neurons [11]; T box brain 2 (Tbr2, rabbit IgG, 1:500, Abcam, Cambridge, UK), a transcription factor that is expressed in the type-2 progenitor cells [21]; glial fibrillary acidic protein (GFAP, clone GA5, mouse IgG_1, 1:200, Millipore Corporation, Temecula, CA, USA), an intermediate filament that is expressed not only in astrocytes but also type-1 progenitor cells [11]; reelin (clone G10, mouse IgG_1, 1:1000; Novus Biologicals, Inc., Littleton, CO, USA), a secreted extracellular matrix glycoprotein that plays a critical role in neuronal migration and positioning during brain development [13]; neuron-specific nuclear protein (NeuN; clone A60, mouse IgG_1, 1:100, Millipore Corporation, Temecula, CA, USA), which specifically detects post-mitotic neurons [22]; glutamic acid decarboxylase 67 (GAD67; clone 1G10.2, mouse IgG_{2a}, 1:50, Millipore Corporation), a GABA-synthesizing enzyme that is expressed in GABAergic neurons [23]; and proliferating cell nuclear antigen (PCNA; clone PC10, mouse IgG_{2a}, 1:200, Dako, Glostrup, Denmark). To quench endogenous peroxidase, the slides were incubated in 0.3% hydrogen peroxide in absolute methanol for 30 min. Immunodetection was carried out using a VECTASTAIN® Elite ABC kit (Vector Laboratories Inc., Burlingame, CA, USA) with 3,3′-diaminobenzidine/H_2O_2 as the chromogen, as previously described [24]. The sections were then counterstained with hematoxylin and coverslipped for microscopic examination.

For evaluation of apoptosis in the SGZ of the dentate gyrus, a terminal deoxynucleotidyl transferase dUTP nick end labeling (TUNEL) assay was applied to brain sections. Deparaffinized sections were treated with 20 μg/mL of proteinase K in phosphate buffered saline (PBS; pH 7.4) for 15 min at room temperature, and then incubated in 3.0% hydrogen peroxide in PBS for 5 min. Detection of apoptotic cells was carried out using the Apop Tag® *in situ* apoptosis detection kit (Millipore Corporation) according to the instructions provided by the manufacturer with 3,3′-diaminobenzidine/H_2O_2 as the chromogen. The same 10 male offspring from eight dams (one or two males per dam) per group at each time point were used for all immunohistochemical studies and the TUNEL assay.

2.7. Morphometry of immunolocalized and apoptotic cells

The SGZ in the dentate gyrus is known for its neurogenesis during development and throughout the postnatal life of granule cells [10,11]. Therefore, DCX-, Tbr2- or GFAP-positive cells as those consisting of granule cell lineage, apoptotic cells as detected by the TUNEL method and proliferating cells as detected by nuclear immunoreactivity of PCNA were bilaterally counted in the SGZ and normalized for the length of the granule cell layer measured as previously described (Fig. 1) [7]. In the hilus of the dentate gyrus, GABAergic interneurons, especially reelin-synthesizing ones, are known to modulate migration and correct positioning of progenitor granule cells [17]. Therefore, reelin- or GAD67-immunoreactive interneurons distributed in the hilus were bilaterally counted and normalized for the number per area unit of the hilar area (polymorphic layer) as previously described (Fig. 1) [7]. We also measured NeuN-positive neurons in the hilus as those of postmitotic interneurons fluctuating in the number in response to aberrant neurogenesis or neuronal mismigration [7]. Large-sized CA3 neurons distributed in this area were easily distinguished from hilar interneurons and excluded from counting as previously described (Fig. 1) [7]. For quantitative measurement of each immunoreactive

Please cite this article in press as: Ohishi T, et al. Reversible aberration of neurogenesis affecting late-stage differentiation in the hippocampal dentate gyrus of rat offspring after maternal exposure to manganese chloride. Reprod Toxicol (2012), http://dx.doi.org/10.1016/j.reprotox.2012.04.009

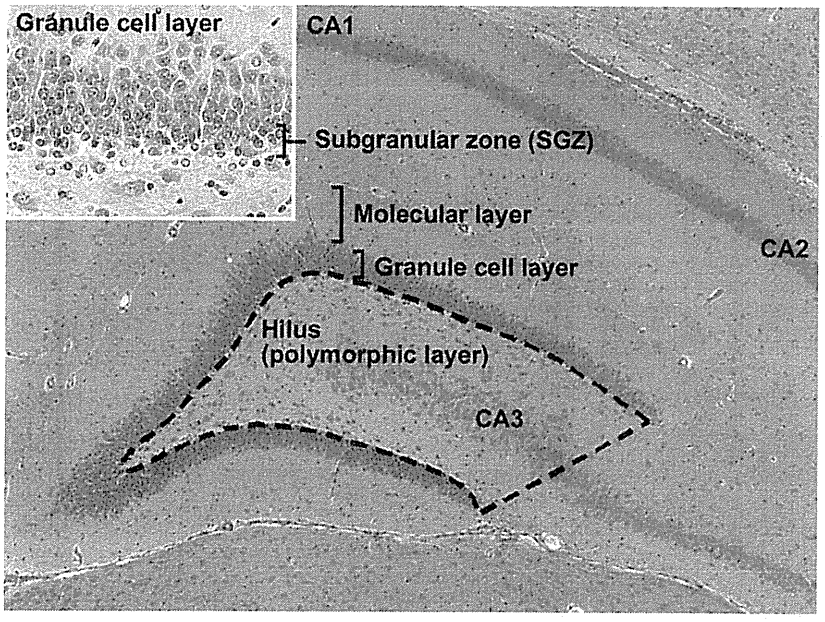

Fig. 1. Overview of the hippocampal formation of a male rat at PND 21 stained with hematoxylin and eosin. The numbers of cells in the hilus of the dentate gyrus (as demarcated by the dotted line) displaying immunoreactivity for reelin, GAD67, and NeuN were counted and normalized for the unit area. Positive immunoreactivity for these antigens was restricted to small-sized neurons in this area, as larger CA3 neurons were not immunoreactive. Magnification, ×40. (Inset) Higher magnification of the granular cell layer and SGZ. Distribution of immunoreactive cells for DCX, Tbr2 and GFAP as well as apoptotic cells and proliferating cells was measured in the SGZ. Magnification, ×400.

cellular component, digital photomicrographs at ×100 magnification were taken using a BX51 microscope (Olympus Optical Co., Ltd., Tokyo, Japan) attached to a DP70 Digital Camera System (Olympus Optical Co.). Quantitative measurements were performed using the WinROOF image analysis software package (version 5.7, Mitani Corp., Fukui, Japan).

2.8. Real-time RT-PCR analysis

For real-time RT-PCR analyses, the cerebrum of male offspring was removed at pre-pubertal necropsy on PND 21 ($n = 5$ or 6/group) and was fixed with methacarn solution for 8 h at 4 °C [25]. Then the hippocampus was removed and stored in ethanol at −80 °C. Analysis of mRNA levels for molecules shown in Supplementary Table 2 was performed with real-time RT-PCR in the hippocampal tissues. *Dcx*, *Neurod1*, *Pax6* and *Dpysl3* were genes encoding neuronal-stage defining marker molecules [21,26,27]. *Reln*, *Vldlr*, *Lrp8* and *Dab1* were genes encoding reelin and its receptors (*Vldlr*, *Lrp8*) and intracellular adaptor (*Dab1*) [28]. Total RNA was extracted using the RNeasy Mini Kit (QIAGEN, Hilden, Germany) according to the manufacturer's instructions. First-strand cDNA was synthesized from 2 μg of total RNA in the presence of dithiothreitol, deoxynucleoside triphosphate (dNTP), random primers, RNaseOUT and SuperScript™ III Reverse Transcriptase (Invitrogen Corp.) in a 20-μL total reaction mixture. Real-time PCR was performed using the SYBR®Green PCR Master Mix (Applied Biosystems Japan Ltd., Tokyo, Japan) and the ABI Prism 7000 Sequence Detection System (Applied Biosystems Japan Ltd.) according to the manufacturer's protocol. The PCR primers shown in Supplementary Table 2 were designed using Primer Express software (Version 3.0; Applied Biosystems Japan Ltd.). The relative differences in gene expression were calculated using threshold cycle (C_T) values that were first normalized to those of the beta-actin gene, the endogenous control in the same sample, and then relative to a control C_T value by the $2^{-\Delta\Delta C_T}$ method [29].

2.9. Statistical analysis

Maternal data regarding body weight, food consumption, Mn concentration in the brain and hormonal analysis were analyzed using the individual animal as the experimental unit. Data for offspring regarding body weight, food consumption, organ weight at necropsy, quantitative data of behavioral examinations, immunohistochemical data, TUNEL-assay data, real-time RT-PCR analysis, Mn concentration in the brain and hormonal analysis were analyzed using the litter as the experimental unit. Differences between the control and each treated group were evaluated using the following methods. Bartlett's test for equal variance was used to determine if the variance was homogenous between the groups. If the variance was homogenous, numerical data were assessed using Dunnett's test to compare between the control and each treated groups. If a significant difference in variance was observed, Steel's test was used instead. Frequency data from behavioral examinations were analyzed using the individual animal as the experimental unit. The number of animals that showed normal reflexes was compared statistically using Fisher's exact test.

3. Results

3.1. Maternal parameters in Experiment 1

There were no statistically significant differences in the body weight during the gestational and lactation periods (Fig. 2). For food consumption, there were no statistically significant differences during the gestational period (Fig. 2). Although statistically significant increases were noted on PND 11 at 160 and 800 ppm of Mn exposure, PND 14 at 800 ppm and PND 17 at 160 ppm (Fig. 2) during the lactation period, these were minimal fluctuations.

The $MnCl_2{\cdot}4H_2O$ intakes of dams from GD 10 to PND 21 were 4.05 mg/kg body weight/day for 32 ppm, 20.62 mg/kg body weight/day for 160 ppm and 105.14 mg/kg body weight/day for 800 ppm. In addition, the $MnCl_2{\cdot}4H_2O$ intakes of dams from GD 10 to PND 21 in Experiment 2 were 100.84 mg/kg body weight/day for 800 ppm and 210.04 mg/kg body weight/day for 1600 ppm.

3.2. Body weight, food consumption, external differentiation and organ weights of offspring in Experiment 1

No statistically significant differences were observed between each treatment and the untreated controls in body weight (Fig. 2), food consumption (Supplementary Fig. 2), external differentiation with regard to pinna detachment, eruption of lower incisor, opening of eyelid, opening of vagina, and cleavage of the balanopreputial gland (Supplementary Table 3), and organ weights (Supplementary Table 4) of offspring after birth through to PND 77.

3.3. Brain Mn-concentration in dams and offspring in Experiment 1

In dams examined on the day 21 after delivery, there were no statistically significant differences in Mn concentration in the

Please cite this article in press as: Ohishi T, et al. Reversible aberration of neurogenesis affecting late-stage differentiation in the hippocampal dentate gyrus of rat offspring after maternal exposure to manganese chloride. Reprod Toxicol (2012), http://dx.doi.org/10.1016/j.reprotox.2012.04.009

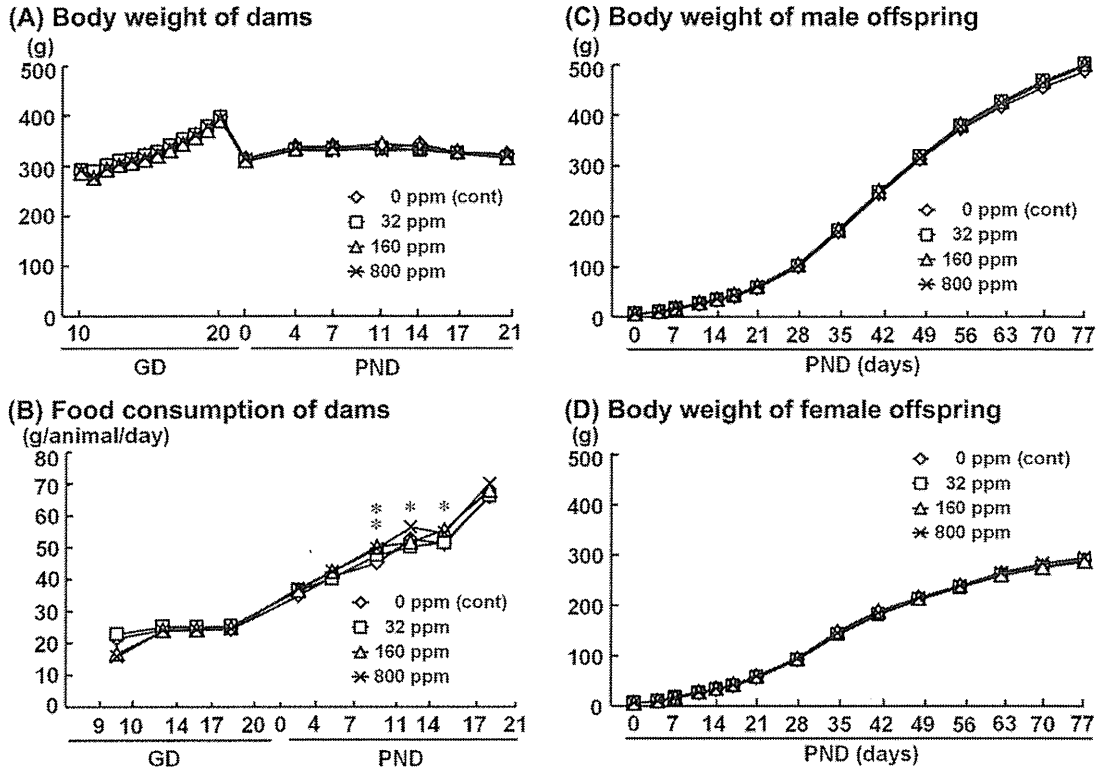

Fig. 2. Body weights and food consumption of dams and body weight of offspring exposed to $MnCl_2{\cdot}4H_2O$ from GD 10 through to day 21 after delivery. (A) Body weight of dams. (B) Food consumption of dams. (C) Body weight of male offspring. (D) Body weight of female offspring. *Significantly different from the untreated controls by Dunnett's test or Steel's test ($P < 0.05$).

cerebellum between the untreated controls and any treatment groups (Fig. 3). In offspring on PND 21, statistically significant increases in Mn concentrations in the cerebellum were observed at 160 and 800 ppm of $MnCl_2{\cdot}4H_2O$ exposure (Fig. 3). In offspring on PND 77, there were no statistically significant differences in Mn concentration in the cerebellum between the untreated controls and any of the treatment groups (Fig. 3).

3.4. Serum concentrations of thyroid-related hormones in Experiment 2

In dams, there were no statistically significant differences in serum concentrations of T_3, T_4 and TSH between the untreated controls and any of the treatment groups (Fig. 4). In offspring on PND 21, statistically significant decreases in serum concentrations of T_3 and T_4 were observed at 800 and 1600 ppm of $MnCl_2{\cdot}4H_2O$ exposure. Although a statistically significant increase was observed in serum concentration of TSH at 800 ppm, no significant change was observed in that at 1600 ppm (Fig. 4). In offspring on PND 77, there were no statistically significant differences in serum concentrations of T_3, T_4 and TSH between the untreated controls and any of the treatment groups (Fig. 4).

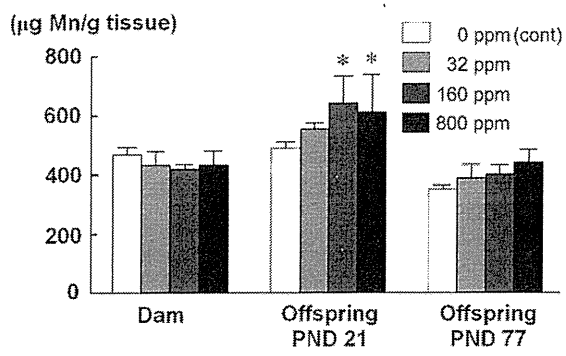

Fig. 3. Manganese concentrations in the cerebellum of dams and male offspring at PND 21 and 77 after maternal exposure to $MnCl_2{\cdot}4H_2O$ from GD 10 to PND 21. All eight dams and six male offspring (one animal per dam) were subjected to analysis in each group. *Significantly different from the untreated controls group by Dunnett's test ($P < 0.05$).

3.5. Behavioral examinations in offspring in Experiment 1

Results of sensory and reflex functional examinations are shown in Table 2. In the surface righting reflex, although a statistically significant lower value was recorded in males at 32 ppm of $MnCl_2{\cdot}4H_2O$ exposure, there were no changes in males at 160 and 800 ppm and in females at all doses. In the air righting reflex, statistically significant lower values were observed in males at 160 ppm or more and in females at 800 ppm. As for the pupillary reflex, Preyer's reflex and pain reflex, all animals showed normal responses in untreated control and all treatment groups.

Results of measurement of grip strength are shown in Table 3. In males, although a statistically significant lower value for the forelimb was recorded at 32 and 160 ppm of $MnCl_2{\cdot}4H_2O$ exposure, there were no changes at 800 ppm. In females, there were no statistically significant differences between the untreated controls and any of the treatment groups.

Results of water-filled multiple T-maze tests are shown in Fig. 5. A statistically significant shortening of the elapsed time was recorded at the 1st trial on the 2nd day in males at 800 ppm of $MnCl_2{\cdot}4H_2O$ exposure. In females, a statistically significant

Please cite this article in press as: Ohishi T, et al. Reversible aberration of neurogenesis affecting late-stage differentiation in the hippocampal dentate gyrus of rat offspring after maternal exposure to manganese chloride. Reprod Toxicol (2012), http://dx.doi.org/10.1016/j.reprotox.2012.04.009

Table 2
Functional examination of offspring exposed to $MnCl_2 \cdot 4H_2O$ during the second half of gestation and lactation periods.

		0 ppm (control)	$MnCl_2 \cdot 4H_2O$ in the diet		
			32 ppm	160 ppm	800 ppm
Males					
No. of offspring examined[a]		16	16	16	16
Surface righting reflex (PND 10, unit: s)		1.7 ± 0.7[b]	1.1 ± 0.3*	1.9 ± 1.0	1.3 ± 0.2
Air righting reflex (PND 15)	Normal	12	7	6#	4##
Pupillary reflex (PND 21)	Normal	16	16	16	16
Preyer's reflex (PND 21)	Normal	16	16	16	16
Pain reflex (PND 21)	Normal	16	16	16	16
Females					
No. of offspring examined[a]		16	16	16	16
Surface righting reflex (PND 10, unit: s)		1.8 ± 0.8	2.3 ± 2.0	1.7 ± 0.8	2.0 ± 1.4
Air righting reflex (PND 15)	Normal	10	8	5	3#
Pupillary reflex (PND 21)	Normal	16	16	16	16
Preyer's reflex (PND 21)	Normal	16	16	16	16
Pain reflex (PND 21)	Normal	16	16	16	16

Abbreviation: PND, postnatal day.
[a] Two male and female offspring per dam were subjected to examination.
[b] Mean ± SD.
* Significantly different from the untreated controls by Dunnett's test or Steel's test ($P < 0.05$).
# Significantly different from the control group by Fisher's exact test ($P < 0.05$).
Significantly different from the control group by Fisher's exact test ($P < 0.01$).

prolongation of the elapsed time and increased counts of error were recorded at the 1st trial on the 2nd day at 800 ppm.

Results from the detailed clinical observations are shown in Supplementary Tables 5–7. There were no differences between the untreated controls and any of the treatment groups for any of these items. Results of manipulative tests are shown in Supplementary Table 8. In the auditory response, approach response, touch response, tail pinch response, pupillary reflex or aerial righting reflex, all animals showed normal responses in the control and all treated groups. In the landing foot splay, there were no statistically significant differences between the untreated controls and any of the treatment groups. Results of measurement of motor activity are shown in Supplementary Table 9. There were no statistically significant differences between the untreated controls and any of the treatment groups.

3.6. Morphometry of immunolocalized cells in the SGZ in Experiment 1

DCX expression was observed in the cytoplasm of many cells located within the SGZ (Fig. 6A). Tbr2 expression was observed in the nucleus of a small number of cells located within the SGZ (Fig. 6B). Immunoreactivity for GFAP was observed in the cytoplasm of a small number of cells located at a lower most portion of the SGZ (Fig. 6C). GFAP expression was also observed in the astrocytes.

On PND 21, a slight but statistically significant increase was observed in the number of DCX-positive cells in the SGZ at 800 ppm of Mn exposure (Fig. 6). As for the number of Tbr2- and GFAP-positive cells in the SGZ, there were no statistically significant differences between the untreated controls and any of the treatment groups (Fig. 6). On PND 77, no statistically significant differences were observed in the number of DCX-, Tbr2- and GFAP-positive cells in the SGZ (Fig. 6).

3.7. Morphometry of immunolocalized cells in the dentate hilus in Experiment 1

Reelin expression was observed in the cytoplasm of neurons located within the hilus of the dentate gyrus, similar to the previous reports [7] (Fig. 7). Immunoreactivity for NeuN was observed in the nucleus of neurons located within the dentate hilus. NeuN-positive neurons were also observed in the nucleus of granule cells, showing cytoplasmic immunoreactivity in addition to nuclear immunolocalization, as reported by others [30]. GAD67-expression was observed in the cytoplasm of the neurons located within the hilus and those sparsely distributed in the granule cell layer.

On PND 21, a slight but statistically significant increase was observed in the number of reelin-positive cells in the hilus at 800 ppm of Mn exposure (Fig. 7). As for the number of NeuN- and GAD67-positive cells in the hilus, there were no statistically significant differences in any of the treatment groups (Fig. 7). On PND 77,

Table 3
Grip strength of offspring exposed to $MnCl_2 \cdot 4H_2O$ during the second half of gestation and lactation periods.

	0 ppm (control)	$MnCl_2 \cdot 4H_2O$ in the diet		
		32 ppm	160 ppm	800 ppm
Males				
No. of offspring examined[a]	8	8	8	8
Forelimb (g)	1347 ± 157[b]	1170 ± 123*	1113 ± 149**	1216 ± 139
Hindlimb (g)	879 ± 205	810 ± 130	703 ± 248	755 ± 120
Females				
No. of offspring examined[a]	8	8	8	8
Forelimb (g)	1050 ± 98	1078 ± 49	1162 ± 160	1107 ± 75
Hindlimb (g)	741 ± 62	719 ± 137	822 ± 107	787 ± 71

[a] One male and female offspring per dam were subjected to examination.
[b] Mean ± SD.
* Significantly different from the untreated controls by Dunnett's test or Steel's test ($P < 0.05$).
** Significantly different from the untreated controls by Dunnett's test or Steel's test ($P < 0.01$).

Please cite this article in press as: Ohishi T, et al. Reversible aberration of neurogenesis affecting late-stage differentiation in the hippocampal dentate gyrus of rat offspring after maternal exposure to manganese chloride. Reprod Toxicol (2012), http://dx.doi.org/10.1016/j.reprotox.2012.04.009

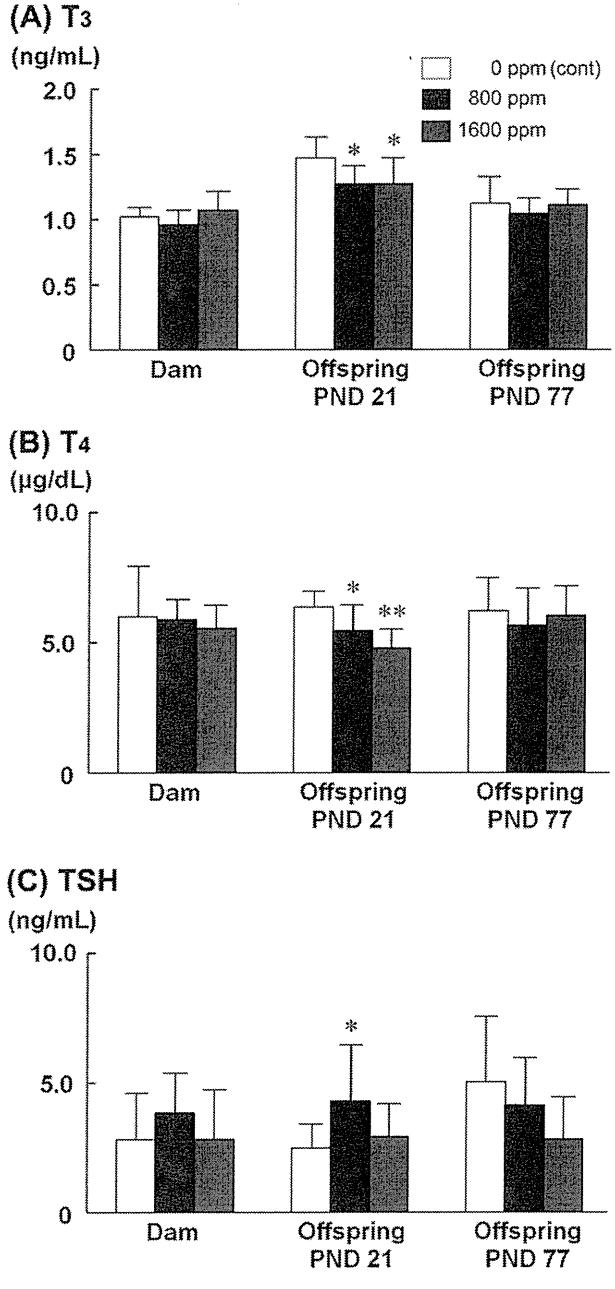

Fig. 4. Serum concentrations of thyroid-related hormones of dams and male offspring at PND 21 and 77 after maternal exposure to $MnCl_2{\cdot}4H_2O$ from GD 10 to PND 21. All six dams and 10 male offspring (one or two animals per dam) were subjected to hormone analysis in each group. Statistical analysis was performed using the litter as the experimental unit, and litter mean values were subjected to analysis on two offspring samples from the same dam. *Significantly different from the untreated controls by Dunnett's test or Steel's test ($P<0.05$). **Significantly different from the untreated controls by Dunnett's test or Steel's test ($P<0.01$).

no statistically significant differences were observed in the number of reelin-, NeuN- and GAD67-positive cells in the hilus (Fig. 7).

3.8. Apoptotic and proliferating cell indices in the dentate SGZ in Experiment 1

On PND 21 and 77, there were no statistically significant differences in the number of TUNEL-positive apoptotic cells and PCNA-positive cells in the SGZ between the untreated controls and any of the treatment groups (Fig. 8).

3.9. Real-time RT-PCR analysis in the hippocampus in Experiment 1

To examine the transcript levels of the molecules related to neuronal development, mRNA levels of *Dcx*, *Neurod1*, *Pax6* and *Dpysl3* in the hippocampus of offspring on PND 21 were analyzed by real-time RT-PCR. *Dcx*, *Neurod1*, *Pax6* and *Dpysl3* did not alter transcript levels in any of the treatment groups (Supplementary Table 10). Furthermore, to investigate the transcript levels of reelin and related molecules, mRNA levels of *Reln*, *Vldlr*, *Lrp8* and *Dab1* in the hippocampus of offspring on PND 21 were analyzed. *Reln*, *Vldlr*, *Lrp8* and *Dab1* did not alter transcript levels in any of the treatment groups (Supplementary Table 10).

4. Discussion

In the present study, supplemental Mn intakes of dams calculated from the $MnCl_2{\cdot}4H_2O$ intake were 1.13 mg/kg body weight/day for 32 ppm, 5.73 mg/kg body weight/day for 160 ppm, 29.21 mg/kg body weight/day for 800 ppm and 58.37 mg/kg body weight/day for 1600 ppm. However, the rodent basal diet contained high concentrations of Mn (7.27 mg/100 g CRF-1 basal diet). This dietary Mn level was equivalent to the Mn intake of 8.94 mg/kg body weight/day from GD 10 to PND 21 in dams of untreated controls. Therefore, total Mn intakes of dams were estimated 10.34 mg/kg body weight/day for 32 ppm, 15.10 mg/kg body weight/day for 160 ppm, 38.76 mg/kg body weight/day for 800 ppm and 67.91 mg/kg body weight/day for 1600 ppm. The ESADDI of Mn has been estimated to be approximately 0.6 mg/day at 7–12 months of age, 1.2 mg/day at 1–3 years of age, 1.5 mg/day at 4–8 years of age and 2–5 mg/day for adults. For newborns, the ESADDI has been estimated to be 0.003 mg/day, less than that for adults or children [1,3]. Therefore, rodent studies are performed with extremely high basal Mn-intake levels as compared with human counterparts. Even when adult value is converted into a measure of mg/kg of body weight (as 50 kg), the daily Mn intake is between 0.04 and 0.1 mg/kg body weight/day. At the lowest dose in the present study, total Mn intake was approximately 100 times higher than the ESADDI in adult humans. Mn-exposure resulted in no major changes in dams except for slight and sporadic increases in food consumption. Offspring also showed no changes in body weight, food consumption and organ weight through to PND 77. However, offspring revealed slight increases in the cellular distribution of DCX- and reelin-positive cells in the dentate gyrus of the hippocampus with Mn exposure at 800 ppm, as well as an increase in the brain Mn concentration at 160 ppm, changes in serum concentrations in thyroid hormones at 800 and 1600 ppm at the end of exposure on PND 21, and changes in reflex functional testing and maze tests at 160 ppm.

Maternal Mn exposure affected the cellular distribution of immunoreactivity for DCX in the SGZ on PND 21 at 800 ppm. Although DCX is expressed in the type-2b and type-3 progenitor cells and immature neurons [11], there were no changes in the numbers of Tbr2-positive cells, suggestive of the type-2 progenitor cells [21]. Therefore, it was considered that type-2b cells were not involved in the increased population of DCX-positive cells, suggestive of an increase in the type-3 progenitor cells or immature granule cells. On the other hand, an increase in the cellular distribution of immunoreactivity for reelin in the dentate hilus also was observed on PND 21 at 800 ppm. Reelin secreted from GABAergic interneurons plays a role for regulating postnatal neurogenesis in the hippocampal dentate gyrus, causing an increase

Please cite this article in press as: Ohishi T, et al. Reversible aberration of neurogenesis affecting late-stage differentiation in the hippocampal dentate gyrus of rat offspring after maternal exposure to manganese chloride. Reprod Toxicol (2012), http://dx.doi.org/10.1016/j.reprotox.2012.04.009

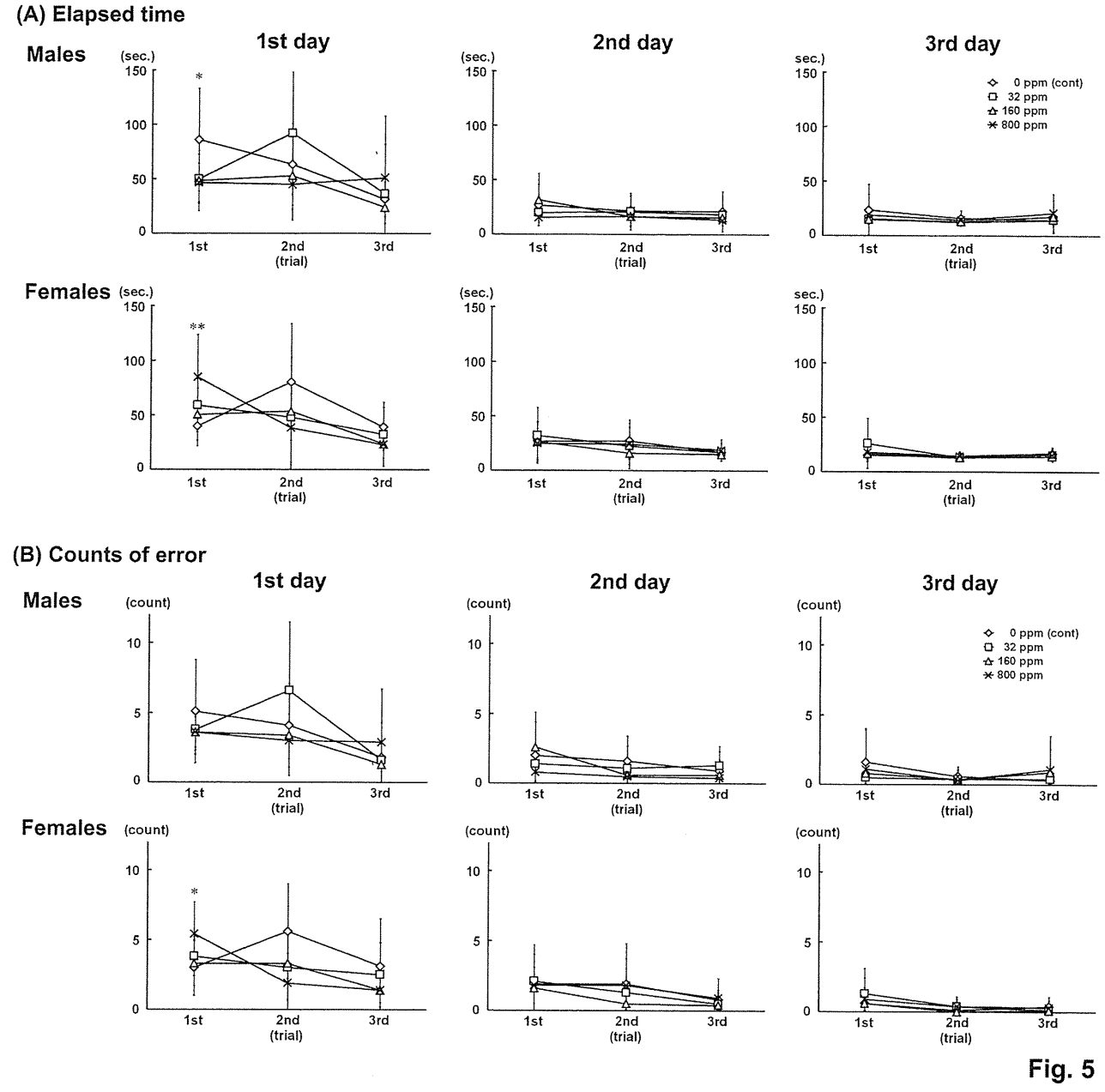

Fig. 5

Fig. 5. Water-filled multiple T-maze test conducted on PND 55, 56 and 57 in offspring after maternal exposure to $MnCl_2 \cdot 4H_2O$ from GD 10 to PND 21. Eight male and eight female offspring (one male and one female animals per dam) were subjected to the examination in each group. (A) Elapsed time. (B) Counts of error. * Significantly different from the untreated controls by Dunnett's test or Steel's test ($P < 0.05$. ** Significantly different from the untreated controls by Dunnett's test or Steel's test ($P < 0.01$).

in DCX-positive immature granule cells [31]. Reelin can also be induced during the course of aberration in the postnatal neurogenesis by developmental exposure to methylazoxymethanol, anti-thyroid agents, or acrylamide in rats [7,18,32]. Therefore, increase of reelin-expressing cells by developmental Mn-exposure may be the reflection of an upregulation of reelin in the GABAergic interneurons causing increased DCX-positive cells, reflecting an aberration in the differentiation of the granule cells. Interestingly, an *in vitro* study using astrocyte–neuron co-cultures has shown that $MnCl_2$ inhibited the ability of astrocytes to promote the neurite outgrowth of hippocampal neuronal precursor cells [33]. This result might be related to the increase of DCX-positive cells in the SGZ found in the present study. Because immature granule cells already have dendritic growth cones and recurrent basal dendrites [34], it might be possible that type 3 progenitor cells is the target of Mn to suppress differentiation to immature granule cells. However, these changes were not observed on PND 77 and were reversible. While immunohistochemical analysis revealed increase of cells positive for DCX or reelin, real-time RT-PCR analysis did not show changes in the transcript levels of the molecules including *Dcx* and *Reln* in the present study. Considering the use of the whole hippocampal tissue including cornu ammonis in the real-time RT-PCR analysis, the changes observed in the substructures, such as the SGZ or dentate hilus, could not be detected.

Please cite this article in press as: Ohishi T, et al. Reversible aberration of neurogenesis affecting late-stage differentiation in the hippocampal dentate gyrus of rat offspring after maternal exposure to manganese chloride. Reprod Toxicol (2012), http://dx.doi.org/10.1016/j.reprotox.2012.04.009

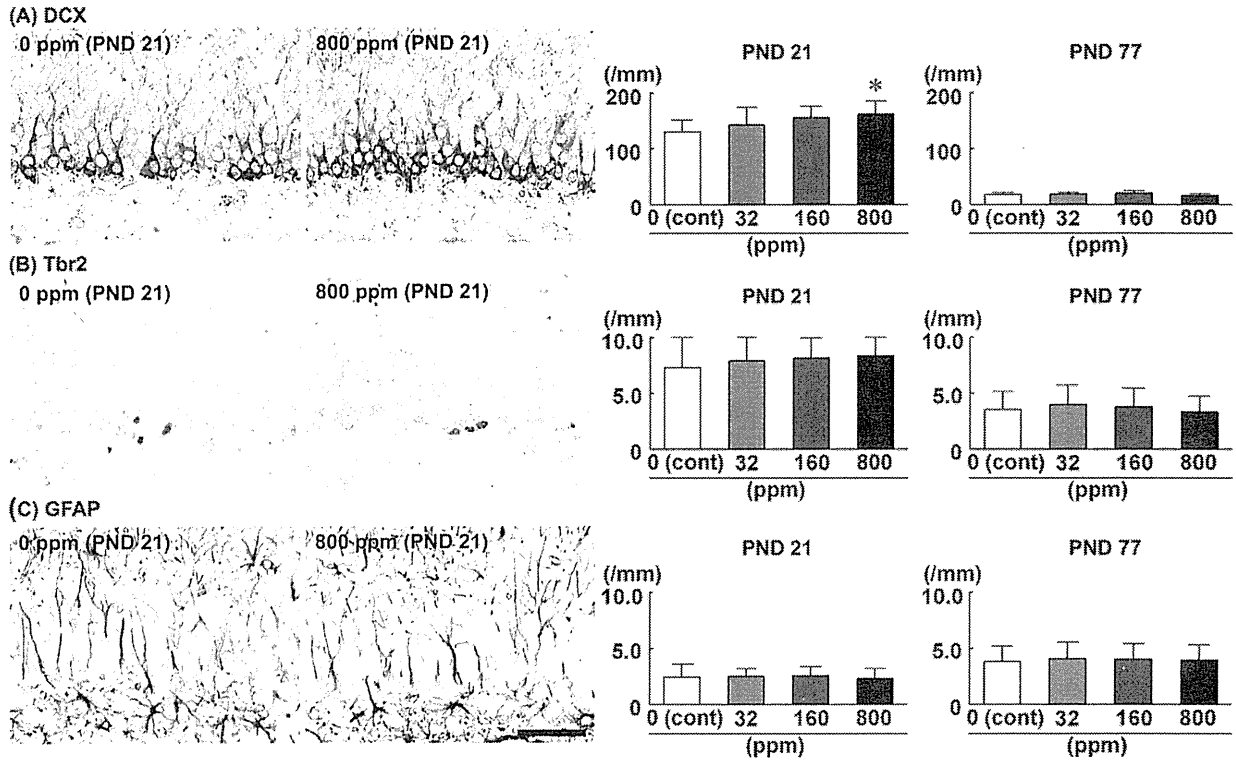

Fig. 6. Distribution of immunoreactive cells for DCX, Tbr2 and GFAP in the dentate subgranular zone of male offspring at PND 21 and 77 after maternal exposure to $MnCl_2 \cdot 4H_2O$ from GD 10 to PND 21. All identical 10 male offspring from eight dams (one or two animals per dam) were subjected to immunohistochemical analyses in each group. (A) DCX. (B) Tbr2. (C) GFAP. Representative images from 0 ppm group (left) and from 800 ppm group (right) at PND 21 (bar = 50 μm). *Significantly different from the untreated controls by Dunnett's test ($P < 0.05$).

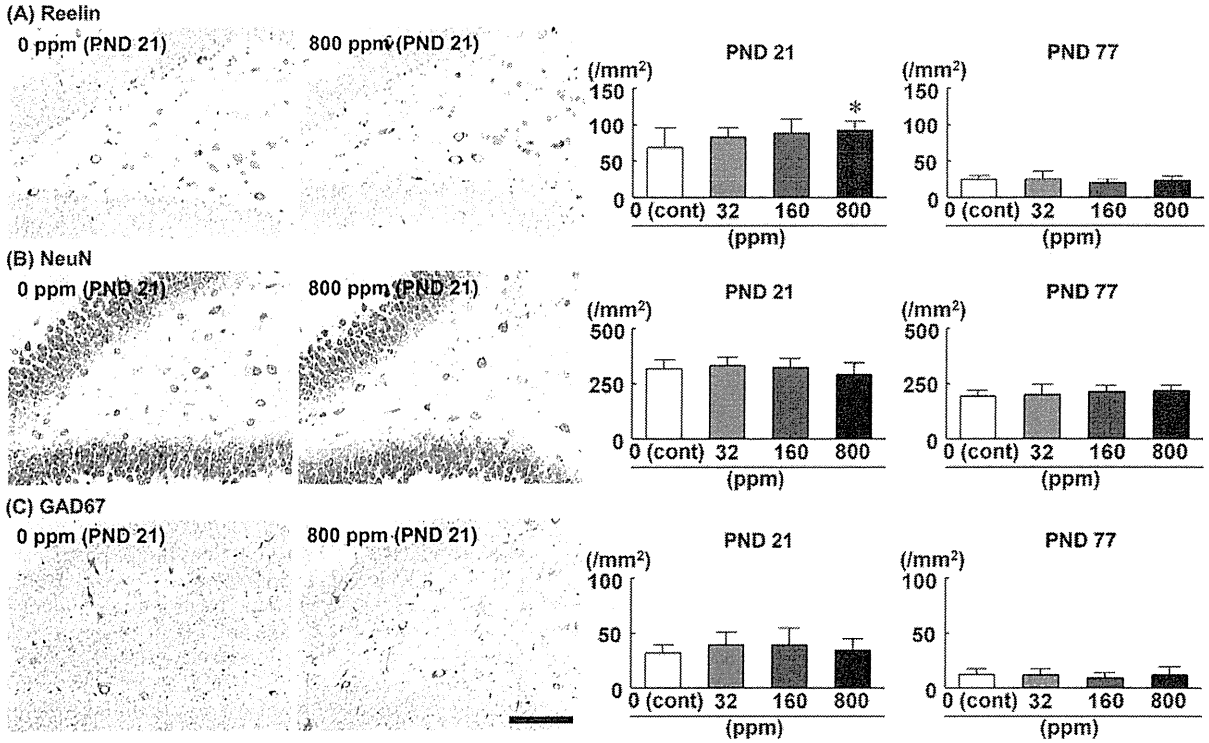

Fig. 7. Distribution of immunoreactive cells for reelin, NeuN and GAD67 in the hilus of the hippocampal dentate gyrus in male offspring at PND 21 and 77 after maternal exposure to $MnCl_2 \cdot 4H_2O$ from GD 10 to PND 21. All identical 10 male offspring from eight dams (one or two animals per dam) were subjected to immunohistochemical analyses in each group. (A) Reelin. (B) NeuN. (C) GAD67. Representative images from 0 ppm group (left) and from 800 ppm group (right) at PND 21 (bar = 100 μm). * Significantly different from the untreated controls by Dunnett's test ($P < 0.05$).

Please cite this article in press as: Ohishi T, et al. Reversible aberration of neurogenesis affecting late-stage differentiation in the hippocampal dentate gyrus of rat offspring after maternal exposure to manganese chloride. Reprod Toxicol (2012), http://dx.doi.org/10.1016/j.reprotox.2012.04.009

Air righting reflex indices in males at 160 ppm of Mn exposure or more and in females at 800 ppm were lower than those in the untreated controls. Tran et al. reported that neonatal rats exposed to high dietary Mn revealed prolongation in the surface righting test [35]. Therefore, a decreased index for the air righting reflex may be the effect of Mn exposure. However, we did not find any effects in other sensory and reflex functional examinations including the surface righting reflex. Therefore, we could not judge that reflex functions were affected by developmental Mn exposure. In addition, water-filled multiple T-maze testing at the 1st trial on the 2nd day (1st day for the T-maze course) revealed shortening of the elapsed time in males and prolongation of the elapsed time and increased counts of error in females at 800 ppm of Mn exposure. However, they were judged to be incidental fluctuations because the changes were almost within the range of three trials in the untreated controls; there were no changes at other trials on all days and there were opposite changes between males and females. Thus, we suggest no apparent effects of developmental Mn exposure on the behavioral examinations including those for learning and memory functions.

In the present study, Mn concentrations in the brain as represented by cerebellar tissue revealed increases in offspring at 160 and 800 ppm at the end of Mn exposure on PND 21, despite no changes in the dams. It is reported that exposure *in utero* and during lactation to inhaled $MnSO_4$ revealed increased Mn concentrations in the striatum and cerebellum of offspring at dose levels showing no changes of Mn concentrations in the dams [36]. In several studies of experimental exposure to $MnCl_2$, Mn concentrations in the brain in developing rats were higher than those concentrations in adult rats at the same dose levels [4,37]. Mn exposure *via* maternal milk from PND 4 to 21 caused Mn accumulation in the cerebellum, midbrain, striatum, cortex and hippocampus in the offspring [38]. Dorman et al. suggested that the increases in brain Mn concentrations might be related to increased Mn absorption from the juvenile gastrointestinal tract, as well as an incompletely formed neonatal blood–brain barrier and a virtual absence of excretory mechanisms until weaning [4]. Also, most Mn salts can penetrate readily the placenta and is toxic to the embryos [39]. These findings suggest that the both fetuses and neonates are rather unprotected against developmental Mn exposure, in contrast to adult animals that have protective functions against ingested Mn even at high doses. Therefore, only the offspring can be exposed to the risk of the neurotoxicity including impaired neuronal differentiation by maternal Mn exposure at high doses.

In the present study, we found decreases in serum concentrations in T_3 and T_4, while serum TSH concentrations increased only at 800 ppm of Mn in offspring at the end of exposure on PND 21. It is reported treatment of rats with a Mn-rich diet ($MnSO_4$) for 5 weeks resulted in decreases in serum T_3, T_4 and TSH concentrations [5]. Also, a 2-year study of Mn exposure in mice revealed thyroid follicular hyperplasia and dilatation, suggestive of the anti-thyroid action of administered Mn [5]. Thyroid hormones play a crucial role in brain development [6]. Experimentally, developmental hypothyroidism leads to neurological defects and impaired performance in a variety of behavioral learning tests [40,41]. The offspring of rats exposed to anti-thyroid agents such as 6-propyl-2-thiouracil show impaired brain development, with aberrant neuronal migration and white matter hypoplasia involving limited axonal myelination and reduced oligodendrocytic distribution [42,43]. In our recent study, the offspring of rats exposed to anti-thyroid agents during development revealed an increase in reelin-synthesizing GABAergic interneurons in the dentate hilus with an immature phenotype that was sustained into the later stage at PND 77 [7]. These results suggested a compensatory mechanism for the impaired neurogenesis and mismigration during neuronal development. Therefore, developmental Mn exposure at high doses might have affected the homeostasis of the thyroid hormones in the offspring, influencing neurogenesis. However, this effect was rather mild or essentially lacking because of the absence of the feature of developmental hypothyroidism such as sustained suppression of body growth and delayed physical development that have been observed in our previous study using anti-thyroid agents [6]. Also, it could not be sustained through to PND 77.

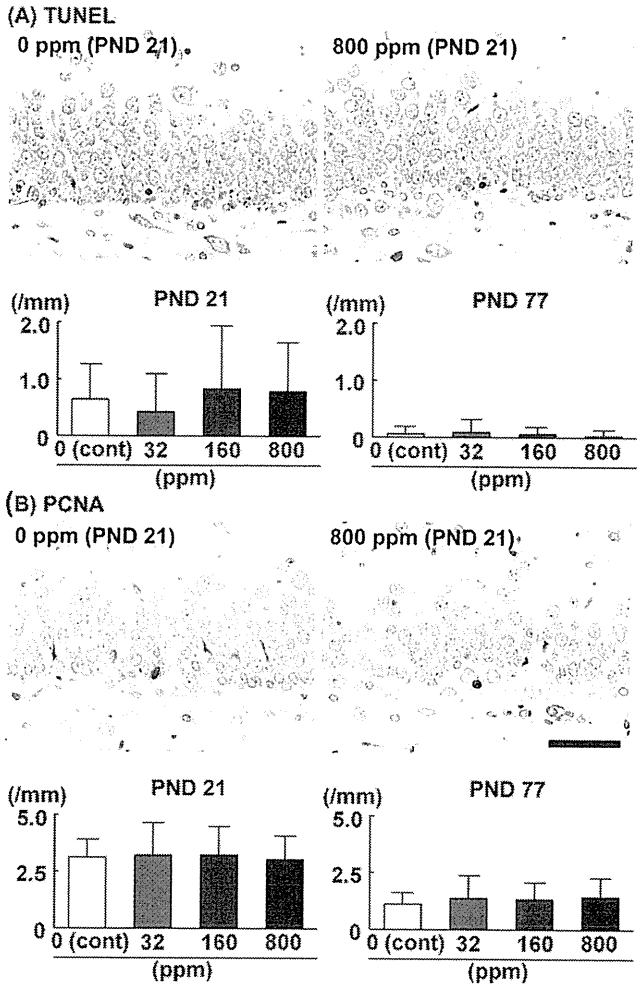

Fig. 8. Distribution of apoptotic cells and proliferating cells in the dentate subgranular zone of male offspring at PND 21 and 77 after maternal exposure to $MnCl_2 \cdot 4H_2O$ from GD 10 to PND 21. All identical 10 male offspring from eight dams (one or two animals per dam) as used in the immunohistochemical analysis were subjected to TUNEL-assay and PCNA-immunohistochemistry in each group. Statistical analysis was performed using the litter as the experimental unit and litter mean values were subjected to analysis on two offspring samples from the same dam. (A) TUNEL. (B) PCNA. Representative images from 0 ppm group (left) and from 800 ppm group (right) at PND 21 (bar = 50 μm).

As described above, although the behavioral examinations could not clarify the obvious effects of developmental Mn exposure, monitoring of the cellular distribution in the SGZ and dentate hilus revealed changes suggestive of effects on neuronal development. Hippocampal neurogenesis in the SGZ continues through the life-span period and decreases in depression, posttraumatic stress disorder and Parkinson's disease, and increases in epileptic seizure, ischemia, Alzheimer's disease and Huntington's disease [44,45]. If developmental exposure to xenobiotics affects neurogenesis and risks the brain diseases mentioned above, analysis of distribution changes in neuronal progenitor cells and interneurons in the dentate gyrus in experimental animals may provide a valuable tool

Please cite this article in press as: Ohishi T, et al. Reversible aberration of neurogenesis affecting late-stage differentiation in the hippocampal dentate gyrus of rat offspring after maternal exposure to manganese chloride. Reprod Toxicol (2012), http://dx.doi.org/10.1016/j.reprotox.2012.04.009

for detection of developmental neurotoxicants affecting neurogenesis.

5. Conclusion

In conclusion, we revealed that maternal Mn exposure mildly and reversibly affects neurogenesis targeting late-stage differentiation in the hippocampal dentate gyrus of rat offspring at 800 ppm $MnCl_2{\cdot}4H_2O$ in diet, a level translating to 38.76 mg/kg body weight/day as Mn. This level is 380–970 times larger than the ESADDI in adult humans (0.04 and 0.1 mg/kg body weight/day with 50 kg body weight). Direct effects of accumulated Mn in the developing brain might be implicated in the mechanism of the development of aberrations in neurogenesis; however, indirect effects through thyroid hormone fluctuations might be rather minor.

Conflict of interest statement

All of the authors disclose that there are no conflicts of interest that could inappropriately influence the outcomes of the present study.

Acknowledgments

This work was supported in part by Health and Labour Sciences Research Grants (Research on Risk of Chemical Substances) from the Ministry of Health, Labour and Welfare of Japan.

Appendix A. Supplementary data

Supplementary data associated with this article can be found, in the online version, at http://dx.doi.org/10.1016/j.reprotox.2012.04.009.

References

[1] Aschner JL, Aschner M. Nutritional aspects of manganese homeostasis. Molecular Aspects of Medicine 2005;26:353–62.
[2] Dobson AW, Erikson KM, Aschner M. Manganese neurotoxicity. Annals of the New York Academy of Sciences 2004;1012:115–28.
[3] Erikson KM, Syversen T, Aschner JL, Aschner M. Interactions between excessive manganese exposures and dietary iron-deficiency in neurodegeneration. Environmental Toxicology and Pharmacology 2005;19:415–21.
[4] Dorman DC, Struve MF, Vitarella D, Byerly FL, Goetz J, Miller R. Neurotoxicity of manganese chloride in neonatal and adult CD rats following subchronic (21-day) high-dose oral exposure. Journal of Applied Toxicology 2000;20:179–87.
[5] Soldin OP, Aschner M. Effects of manganese on thyroid hormone homeostasis: potential links. Neurotoxicology 2007;28:951–6.
[6] Shibutani M, Woo G-H, Fujimoto H, Saegusa Y, Takahashi M, Inoue K, et al. Assessment of developmental effects of hypothyroidism in rats from in utero and lactation exposure to anti-thyroid agents. Reproductive Toxicology 2009;28:297–307.
[7] Saegusa Y, Woo GH, Fujimoto H, Kemmochi S, Shimamoto K, Hirose M, et al. Sustained production of Reelin-expressing interneurons in the hippocampal dentate hilus after developmental exposure to anti-thyroid agents in rats. Reproductive Toxicology 2010;29:407–14.
[8] Zhang L, Blomgren K, Kuhn HG, Cooper-Kuhn CM. Effects of postnatal thyroid hormone deficiency on neurogenesis in the juvenile and adult rat. Neurobiology of Disease 2009;34:366–74.
[9] Sato N, Hatakeyama S, Shimizu N, Hikima A, Aoki J, Endo K. MR evaluation of the hippocampus in patients with congenital malformations of the brain. American Journal of Neuroradiology 2001;22:389–93.
[10] Eriksson PS, Perfilieva E, Björk-Eriksson T, Alborn AM, Nordborg C, Peterson DA, et al. Neurogenesis in the adult human hippocampus. Nature Medicine 1998;4:1313–7.
[11] Kempermann G, Jessberger S, Steiner B, Kronenberg G. Milestones of neuronal development in the adult hippocampus. Trends in Neurosciences 2004;27:447–52.
[12] Lussier AL, Caruncho HJ, Kalynchuk LE. Repeated exposure to corticosterone, but not restraint, decreases the number of reelin-positive cells in the adult rat hippocampus. Neuroscience Letters 2009;460:170–4.
[13] D'Arcangelo G, Nakajima K, Miyata T, Ogawa M, Mikoshiba K, Curran T. Reelin is a secreted glycoprotein recognized by the CR-50 monoclonal antibody. Journal of Neuroscience 1997;17:23–31.
[14] Houser CR. Interneurons of the dentate gyrus: an overview of cell types, terminal fields and neurochemical identity. Progress in Brain Research 2007;163:217–32.
[15] Pesold C, Impagnatiello F, Pisu MG, Uzunov DP, Costa E, Guidotti A, et al. Reelin is preferentially expressed in neurons synthesizing gamma-aminobutyric acid in cortex and hippocampus of adult rats. Proceedings of the National Academy of Sciences of the United States of America 1998;95:3221–6.
[16] Scotti AL, Herrmann G. Reelin immunoreactivity in dissociated cultures of the postnatal hippocampus. Brain Research 2002;924:209–18.
[17] Gong C, Wang TW, Huang HS, Parent JM. Reelin regulates neuronal progenitor migration in intact and epileptic hippocampus. Journal of Neuroscience 2007;27:1803–11.
[18] Ogawa B, Wang L, Ohishi T, Taniai E, Akane H, Suzuki K, et al. Reversible aberration of neurogenesis targeting late-stage progenitor cells in the hippocampal dentate gyrus of rat offspring after maternal exposure to acrylamide. Archives of Toxicology; in press. Q2
[19] Biel WC. Early age differences in maze performance in the albino rats. Journal of Genetic Psychology 1940;56:439–45.
[20] Hirata-Koizumi M, Fujii S, Ono A, Hirose A, Imai T, Ogawa K, et al. Evaluation of the reproductive and developmental toxicity of aluminium ammonium sulfate in a two-generation study in rats. Food and Chemical Toxicology 2011;49:1948–59.
[21] Hodge RD, Kowalczyk TD, Wolf SA, Encinas JM, Rippey C, Enikolopov G, et al. Intermediate progenitors in adult hippocampal neurogenesis: Tbr2 expression and coordinate regulation of neuronal output. Journal of Neuroscience 2008;28:3707–17.
[22] Mullen RJ, Buck CR, Smith AM. NeuN a neuronal specific nuclear protein in vertebrates. Development 1992;116:201–11.
[23] Wierońska JM, Brański P, Siwek A, Dybala M, Nowak G, Pilc A. GABAergic dysfunction in mGlu7 receptor-deficient mice as reflected by decreased levels of glutamic acid decarboxylase 65 and 67 kDa and increased reelin proteins in the hippocampus. Brain Research 2010;1334:12–24.
[24] Shibutani M, Lee KY, Igarashi K, Woo G-H, Inoue K, Nishimura T, et al. Hypothalamus region-specific global gene expression profiling in early stages of central endocrine disruption in rat neonates injected with estradiol benzoate or flutamide. Developmental Neurobiology 2007;67:253–69.
[25] Shibutani M, Uneyama C, Miyazaki K, Toyoda K, Hirose M. Methacarn fixation: a novel tool for analysis of gene expressions in paraffin-embedded tissue specimens. Laboratory Investigation 2000;80:199–208.
[26] Breunig JJ, Silbereis J, Vaccarino FM, Sestan N, Rakic P. Notch regulates cell fate and dendrite morphology of newborn neurons in the postnatal dentate gyrus. Proceedings of the National Academy of Sciences of the United States of America 2007;104:20558–63.
[27] Knoth R, Singec I, Ditter M, Pantazis G, Capetian P, Meyer RP, et al. Murine features of neurogenesis in the human hippocampus across the lifespan from 0 to 100 years. PLoS One 2010;5:e8809.
[28] Hack I, Hellwig S, Junghans D, Brunne B, Bock HH, Zhao S, et al. Divergent roles of ApoER2 and Vldlr in the migration of cortical neurons. Development 2007;134:3883–91.
[29] Livak KJ, Schmittgen TD. Analysis of relative gene expression data using real-time quantitative PCR and the $2^{-\Delta\Delta C_T}$ method. Methods 2001;25:402–8.
[30] Van Nassauw L, Wu M, De Jonge F, Adriaensen D, Timmermans JP. Cytoplasmic, but not nuclear, expression of the neuronal nuclei (NeuN) antibody is an exclusive feature of Dogiel type II neurons in the guinea-pig gastrointestinal tract. Histochemistry and Cell Biology 2005;124:369–77.
[31] Pujadas L, Gruart A, Bosch C, Delgado L, Teixeira CM, Rossi D, et al. Reelin regulates postnatal neurogenesis and enhances spine hypertrophy and long-term potentiation. Journal of Neuroscience 2010;30:4636–49.
[32] Hoareau C, Hazane F, Le Pen G, Krebs MO. Postnatal effect of embryonic neurogenesis disturbance on reelin level in organotypic cultures of rat hippocampus. Brain Research 2006;1097:43–51.
[33] Giordano G, Pizzurro D, VanDeMark K, Guizzetti M, Costa LG. Manganese inhibits the ability of astrocytes to promote neuronal differentiation. Toxicology and Applied Pharmacology 2009;240:226–35.
[34] Ribak CE, Korn MJ, Shan Z, Obenaus A. Dendritic growth cones and recurrent basal dendrites are typical features of newly generated dentate granule cells in the adult hippocampus. Brain Research 2004;1000:195–9.
[35] Tran TT, Chowanadisai W, Crinella FM, Chicz-DeMet A, Lönnerdal B. Effect of high dietary manganese intake of neonatal rats on tissue mineral accumulation, striatal dopamine levels, and neurodevelopmental status. Neurotoxicology 2002;23(4–5):635–43.
[36] Dorman DC, McElveen AM, Marshall MW, Parkinson CU, James RA, Struve MF, et al. Tissue manganese concentrations in lactating rats and their offspring following combined in utero and lactation exposure to inhaled manganese sulfate. Toxicological Sciences 2005;84:12–21.
[37] Takeda A, Ishiwatari S, Okada S. Manganese uptake into rat brain during development and aging. Journal of Neuroscience Research 1999;56:93–8.
[38] Garcia SJ, Gellein K, Syversen T, Aschner M. A manganese-enhanced diet alters brain metals and transporters in the developing rat. Toxicological Sciences 2006;92:516–25.
[39] Gerber GB, Léonard A, Hantson P. Carcinogenicity, mutagenicity and teratogenicity of manganese compounds. Critical Reviews in Oncology/Hematology 2002;42:25–34.

Please cite this article in press as: Ohishi T, et al. Reversible aberration of neurogenesis affecting late-stage differentiation in the hippocampal dentate gyrus of rat offspring after maternal exposure to manganese chloride. Reprod Toxicol (2012), http://dx.doi.org/10.1016/j.reprotox.2012.04.009

[40] Comer CP, Norton S. Effects of perinatal methimazole exposure on a developmental test battery for neurobehavioral toxicity in rats. Toxicology and Applied Pharmacology 1982;63:133–41.
[41] Akaike M, Kato N, Ohno H, Kobayashi T. Hyperactivity and spatial maze learning impairment of adult rats with temporary neonatal hypothyroidism. Neurotoxicology and Teratology 1991;13:317–22.
[42] Schoonover CM, Seibel MM, Jolson DM, Stack MJ, Rahman RJ, Jones SA, et al. Thyroid hormone regulates oligodendrocyte accumulation in developing rat brain white matter tracts. Endocrinology 2004;145:5013–20.
[43] Goodman JH, Gilbert ME. Modest thyroid hormone insufficiency during development induces a cellular malformation in the corpus callosum: a model of cortical dysplasia. Endocrinology 2007;148:2593–7.
[44] Zhao C, Deng W, Gage FH. Mechanisms and functional implications of adult neurogenesis. Cell 2008;132:645–60.
[45] Abrous DN, Koehl M, Le Moal M. Adult neurogenesis: from precursors to network and physiology. Physiological Reviews 2005;85:523–69.

Please cite this article in press as: Ohishi T, et al. Reversible aberration of neurogenesis affecting late-stage differentiation in the hippocampal dentate gyrus of rat offspring after maternal exposure to manganese chloride. Reprod Toxicol (2012), http://dx.doi.org/10.1016/j.reprotox.2012.04.009

Bull, Natl. Inst. Health Sci., **129**, 105-110 (2011) **Note**

有機リン系化合物クロルピリホスの経胎盤・経母乳暴露が発達期のマウス免疫系に及ぼす影響について

中村亮介#, 木村美恵, 松岡英樹, 蜂須賀暁子, 中村里香, 中村　厚, 渋谷　淳*, 手島玲子

Effects of transplacental and trans-breast milk exposure to the organophosphate compound chlorpyrifos on the developing immune system of mice

Ryosuke Nakamura#, Yoshie Kimura, Hideki Matsuoka, Akiko Hachisuka, Rika Nakamura, Atsushi Nakamura, Makoto Shibutani* and Reiko Teshima

Navarro et al (2001) have reported that neonatal exposure of rat to the organophosphate compound chlorpyrifos (CPF) resulted in long-term deficits in T lymphocyte mitogenic response, although the mechanism has been unclear. In this study, pregnant BALB/c mice were exposed to 0, 2.8, 14, 70ppm CPF via diet from gestational day 10 to postnatal day (PND) 21, and subpopulational changes in T lymphocytes of offspring were analyzed at PND21. The irreversibility of the effects was also investigated at PND77 after ceasing exposure by weaning at PND21. Serum cholinesterase activity was significantly reduced after exposure to CPF at PND21. An increase in the proportion of CD4 positive splenocytes was observed after exposure to CPF, which remained until PND77. We found that regulatory T cells were the only one CD4 positive subset which increased in the spleen of CPF-exposed mice at PND77.

Keywords: organophosphates, chlorpyrifos, developing immune system, CD4 T cells

1. 緒　言

免疫系は，神経系および内分泌系との密接な相互作用を通じ，生体防御に重要な役割を果たしている．これら3つのシステムは発達期における外部環境の影響を受けやすいことが知られており，この感受性の高い時期はしばしば「critical window」とよばれている[1,2]．しかし，従来の免疫毒性試験評価では発達期への影響を検討していない．

シロアリ駆除剤として居室を含有する建築物への使用は禁止されたものの，殺虫剤として使用されるクロルピリホス（CPF）は，有機リン系化合物の一種で，アセチルコリンエステラーゼを阻害して神経伝達物質のアセチルコリン濃度を高めることにより作用を発揮する（Fig. 1）．Navarroらは，新生児ラットに出産後4日間CPFを皮下投与すると，成熟後におけるT細胞のconcanavalin A刺激に対する増殖能が有意に低下したと報告しており[3]，CPFの発達期免疫への影響が疑われているが，そのメカニズムの詳細は明らかになっていない．

細胞性免疫や液性免疫など，適応免疫の型を決定づける上で最も重要な役割を担っているのは細胞表面マーカーCD4を発現するT細胞集団（ヘルパーT細胞；Th）であるが，これは少なくとも4種の機能的に異なるサブセットから構成されており，そのバランスにより免疫反応の型が制御されていることが知られている．すなわち，インターフェロンγ（IFNγ）等を発現し，細胞性免疫に関与するTh1[4]，インターロイキン（IL）4，5

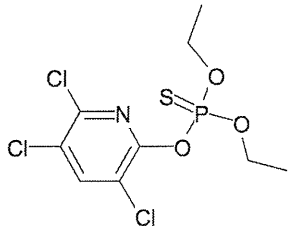

Fig. 1 Structure of chlorpyrifos (CAS#2921-88-2)

To whom correspondence should be addressed:
Ryosuke Nakamura; Division of Novel Foods and Immunochemistry, National Institute of Health Sciences, 1-18-1 Kamiyoga, Setagaya-ku, Tokyo 158-8501 Japan; Tel: +81-3-3700-9437; Fax: +81-3-3707-6950; E-mail: ryosnak@nihs.go.jp
* Tokyo University of Agriculture and Technology

等を発現し，アレルギーや液性免疫に関与するTh2[4]，IL-17を発現し，多くの自己免疫疾患に関与するTh17[5]，そしてIL-10等を発現し，免疫反応の抑制に中心的な役割を果たしている制御性T細胞（regulatory T cell; Treg）[6]の4種である．本研究では，Navarroらがラットにおいて発見したCPFの発達期免疫への影響をより詳細に解析するため，リンパ球のサブポピュレーション解析（$CD4^+$ T細胞，$CD8^+$ T細胞，NK細胞）およびこれら4種の$CD4^+$ T細胞サブセット解析を行い，特に免疫反応の抑制に関与するTregの増加が誘導されている可能性について追究した．

暴露系としては，ラット[7-11]およびマウス[12]を用いて抗甲状腺作用が疑われる化学物質への暴露が発達期の神経系および免疫系に及ぼす影響を簡便にスクリーニングすることに成功した先行研究が存在するため，このプロトコルに則った．具体的には，妊娠マウスを妊娠10日（GD10）から出産後21日（PND21）までCPFに混餌（0，2.8，14，70ppm）投与にて暴露し，暴露終了時での児マウスの解析を行った．また，PND21までの暴露終了後，PND77まで通常飼料による飼育を行い，PND21の時点で認められた変化が11週齢で回復するかどうかを調べた．

2．実験方法

2．1．被験物質

CPFの構造式を図1に示した．CPF（DURSBAN™ XP；M.W.350.6，CAS No.2921-88-2，純度99.8%，通常の保存条件下で安定．弱酸・弱アルカリで安定）はDow AgroSciences社の厚意により分与された．

2．2．試薬

粉末CRF-1は日本チャールスリバー（株）より購入した．次の蛍光標識抗体はBioLegend社より購入した：APC/Cy7標識抗マウスCD3抗体（145-2C11），FITC標識抗マウスCD4抗体（RM4-5），APC標識抗マウスCD8a抗体（53-6.7），PerCP/Cy5.5標識抗マウスIFNγ抗体（XMG1.2），PE標識抗マウスIL-4抗体（11B11），APC標識抗マウスIL-17A抗体（TC11-18H10.1），PerCP/Cy5.5標識（PEおよびAPCも同様）ラットIgG1κアイソタイプコントロール抗体（RTK2071）．PE標識抗マウスCD25抗体（PC61）はBD Pharmingen社より購入した．PE標識抗マウスCD49b抗体（DX5）およびAPC標識抗マウスFoxp3抗体（FJK-16s）はeBioscience社より購入した．Leukocyte Activation Coktail，with BD GolgiPlugおよびBD GolgiPlugはBD Pharmingen社より購入した．

2．3．使用動物

9-11週齢の妊娠2日（GD2；プラグがついた日を妊娠1日と起算）のBALB/cマウスを日本チャールスリバー（株）より購入し，7日間予備飼育後，実験に供した．動物は，GD9までは群飼い（1ケージあたり3匹），GD10からは個別飼育とし，照明12時間，温度24±1℃，湿度55±5%に保たれたバリアシステムの飼育室（SPF）で飼育した．動物実験は国立医薬品食品衛生研究所の規定に準拠し，動物実験委員会の承認に基づき実施した．

2．4．CPFへの暴露

CPFは，粉末CRF-1飼料に0，2.8，14，70ppm（公比5）にて乳鉢，ビニル袋，ポリプロピレン容器を用いて混合し，混餌飼料を調製した．検体は各段階で十分混合しつつ，3段階の段階希釈により得た．検体の濃度は，ラットにおける生殖毒性を検討した過去の報告[13]および血清中コリンエステラーゼ活性の抑制を指標とした用量設定試験により決定した．妊娠2日目（GD2）のBALB/cマウス（9～11週齢）を購入し，1ケージあたり3匹でGD9まで飼育し，GD10より単独飼育にすると同時に粉末CRF-1への混餌投与にてCPFの暴露を開始した（1群12匹）．最終的に，12匹中コントロール群は3匹，暴露群はすべて6匹のマウスが出産に至った．出産後3週目（PND21）まで暴露を継続し，その間体重および摂餌量を計測した．また，出産した児マウスの体重も同様に計測した．児マウスの飼育数は，栄養状態が均等となるよう，9匹以上生まれたケージからは1ケージあたり8匹となるように無作為に間引いて8匹未満の出産ケージに移動し，総数を8匹に揃えた．PND21に同腹から体重が中央値に近い児マウスを選び解剖（雌雄それぞれn＝4）を行った．さらに，雄の児動物については，暴露終了後PND77まで飼育し，被験物質による影響の回復性を調べた．一般状態および体重測定は7日ごとに行った．

2．5．血液学的検査

エーテル深麻酔下のマウス眼底から末梢血30 μlを採取し，120 μlの0.5%EDTA/CELLPAKに懸濁し，多項目自動血球計数装置（M-2000，Sysmex corp.）に供した．解析項目は次の通り：赤血球数（RBC），白血球数（WBC），ヘモグロビン濃度（HGB），ヘマトクリット値（HCT），平均赤血球容積（MCV），平均赤血球血色素量（MCH），平均赤血球血色素濃度（MCHC），および血小板（PLT）．

2．6．血液生化学的検査

母動物および児動物について，末梢血より血清200 μlを採取し，SRL社に委託して次の項目の検査を行った：アルブミン/グロブリン（A/G）比，アスパラギン酸アミノトランスフェラーゼ（AST），アラニンアミノトランスフェラーゼ（ALT），および血清中コリンエス

テラーゼ活性（ChE）．ただし，PNW 3の児動物から採取できる血清はわずかであったため，2匹分の血清試料を1検体にまとめて測定した．その際，PND21群においては雌児の数が十分確保できなかったため，雌2検体に3または4検体の雄を合わせてn＝5または6として検定を行った．

2．7．病理組織学的解析

児マウスについては，肝臓，脾臓，胸腺，および骨髄（大腿骨）における病理組織学的解析を行った．採取組織を定法に従って中性緩衝ホルマリン液で固定し，薄切切片をヘマトキシリン・エオジン染色した．

2．8．フローサイトメトリー

リンパ球のポピュレーション解析を行うため，児マウスの脾臓および胸腺を冷温下でシリンジにより破砕して口径70 μmのメッシュに通し，10 mlの10%FCS(Gibco)を添加したRPMI1640培地に懸濁した．トリパンブルー染色の後，自動細胞数計測装置（Countess；Invitrogen社）により細胞数を計測し，以下に述べる3種の条件により染色を行った．測定にはBectonDickinson社のFACSAriaを用い，データ解析にはFlowJo（トミーデジタルバイオロジー社）を用いた．フローサイトメトリーではtotal event数として10万個の細胞を計測し，各サブセットの存在比率は，特に断らない限り，定法通り前方散乱および側方散乱により定義したリンパ球ゲート内の総リンパ球数に対するパーセンテージとして表した[7,8,10]．

2．8．1．CD 3/CD 4/CD 8 a/CD49bを抗原とするリンパ球サブポピュレーション解析

T細胞およびNK細胞のサブポピュレーションを解析するため，セルストレイナー付き丸底ポリスチレンチューブに細胞を2×10^6cells分注し，成熟T細胞マーカーであるCD3，ヘルパーT細胞のマーカーであるCD4，細胞傷害性T細胞のマーカーであるCD8a，およびNK細胞のマーカーであるCD49bを2.1.に示した抗体により氷上で30分間染色した．

2．8．2．CD 4/IFNγ/IL 4/IL17Aを抗原とするCD 4陽性T細胞サブセット解析

ヘルパーT細胞のサブセットであるTh1/Th2/Th17を染色するため，表面抗原であるCD4とともに，それぞれのマーカーとなる細胞内サイトカインIFNγ/IL-4/IL-17Aを染色した．採取後の細胞を24wellプレートに4×10^6cells/1 ml/wellずつ分注し，PMAとイオノマイシンを含むリンパ球活性化試薬（Leukocyte Activation Coktail，with BD GolgiPlug）によりCO_2インキュベータ中で37℃，4時間刺激し，セルストレイナー付きチューブに回収した．FOXP3Fix/Perm buffer (BioLegend)により室温で30分固定後，CD4を染色，洗浄後にFOXP3Perm bufferで細胞を可溶化し，細胞内サイトカイン抗体で染色した．アイソタイプコントロールとしては，同じ蛍光色素で標識された非特異的ラットIgG1κを用いた．また，未刺激のネガティブコントロールには，BD GolgiPlugのみを用いた．

2．8．3．CD 4/CD25/Foxp 3を抗原とするTreg解析

Tregは，CD4とともに表面マーカーのCD25または核内抗原であるFoxp3により同時染色し解析した．セルストレイナー付きチューブに細胞を2×10^6cells分注し，氷上でCD4/CD25を染色後，FOXP3Fix/Perm bufferセットにより固定・可溶化し，Foxp3を染色した．

2．9．統計処理

有意差の有無に関する統計計算は，Dunnettの方法（n＝4）により，$p<0.05$を有意とした．なお，病理組織学的解析の判定にはFisherの直接確率検定によった．

3．結果および考察

3．1．一般毒性学的影響

母マウスおよび児マウスについて，体重・臓器重量・血液学的検査・血液生化学的検査および病理組織学的解析を行った．なお，CPF暴露群において摂餌量に有意な変化はなく，性比への影響も認められなかった．CPF暴露群においては，一部の母マウスで体重または脾臓重量の増大が認められたが，児については70ppm暴露群の雄において，PND21の胸腺比重量の有意な増大が認められた（Table 1）．しかし，PND77には回復していたことから，その影響はごく軽微にとどまっているものと考えられた．血液学的影響としては，70ppm暴露群の母マウスにおいて白血球の増加と赤血球および各種赤血球関連パラメータの減少が認められたが，児マウスにおいては用量依存性のない軽微な変化のみが認められた（data not shown）．血液生化学的検査のうち，肝機能関連のパラメータ（A/G比，AST，ALT）には有意差は認められなかった（data not shown）．一方，中用量以上のCPF暴露は母親および児に対し，PND21における顕著な血清中コリンエステラーゼ（ブチリルコリンエステラーゼ）阻害を誘導した．このことは，CPFの経胎盤・経乳的暴露が正しく成立していたことを示している．しかし，血清中のコリンエステラーゼ活性の多くはブチリルコリンエステラーゼによるものであり，CPFの神経作用の本態であるアセチルコリンエステラーゼ阻害とは必ずしも対応しないことには注意を要する．実際，立毛や痙攣，運動失調などの所見は認められなかった．PND77の児動物においては活性は回復している．また，児動物の肝臓・脾臓・胸腺・骨髄の病理組織学的